Assessment of methods for reconstructing Little Ice Age glacier surfaces on the examples of Novaya Zemlya and the Swiss Alps

Johannes Reinthaler, Frank Paul

Assessment of methods for reconstructing Little Ice Age glacier surfaces on the examples of Novaya Zemlya and the Swiss Alps

Johannes Reinthaler[1,*], Frank Paul[1]

[1]Department of Geography, University of Zurich, Zurich, Switzerland

*Corresponding author. Winterthurerstrasse 190, 8057 Zürich.

E-mail address: johannes.reinthaler@geo.uzh.ch.

Keywords:

Glacier reconstruction, Little Ice Age, glacier volume change

Abstract

Climate change since the end of the Little Ice Age (LIA) has driven observed glacier volume loss, significantly contributing to the rise of global sea level. The related calculation of volume change requires knowledge of glacier surfaces from at least two points in time, usually represented by two digital elevation models (DEMs). These are typically derived from photogrammetric techniques using stereo images, but such images do not go back to the LIA. Accordingly, several techniques have been developed to reconstruct LIA glacier surfaces from historic outlines and modern DEMs. Here we first evaluate various surface interpolation methods by replicating modern glacier surfaces from outline elevation points and analyse elevation differences and uncertainties. Secondly, we investigate different GIS-based methods for LIA surface reconstruction including a new method that is based on up-scaling of recent glacier-specific elevation change data and works also for ice caps without lateral moraines. The methods were tested on 90 glaciers (covering 643 km^2) in southern Novaya Zemlya and 266 glaciers (524 km^2) in the Bernese Alps of Switzerland. As in previous studies, we also found that the *Natural Neighbor* and *Topo to Raster* interpolation methods in ESRI's ArcGIS performed best for glacier surface reconstruction and that all methods are challenged by replicating the variable surface curvature of glaciers. The new reconstruction method shows the smallest mean difference to the reference dataset (RMSE of 26.7 vs. 39.8 m). The often neglected small surface lowering

in the accumulation area can increase the derived glacier volume changes by 30-50% and should thus be considered whenever possible. Applying the up-scaling method to both test regions revealed that elevation change rates over the last two decades (-0.8 m a^{-1} for Novaya Zemlya and -1.14 m a^{-1} for the Bernese Alps) were much higher than from 1850 until today (-0.13 m a^{-1} and -0.22 m a^{-1}, respectively).

1. Introduction

Glacier melt is a major contributor to current global sea-level rise, with regions such as Alaska, Arctic Canada and the Russian Arctic contributing the most (Horwath et al., 2022; Oppenheimer et al., 2019; Zemp et al., 2019). To calculate this contribution from the volume change (geodetic mass balance) of a glacier, surface elevations at two points in time are necessary. Fortunately, modern digital elevation models (DEMs) provide surface elevations for the entire globe, usually based on optical stereo imagery or interferometric techniques using synthetic aperture radar (SAR). Glacier volume changes on a global scale are available for the last 20 years using elevation information derived from time series of stereo images (Hugonnet et al., 2021). Historical DEMs, however, are rare, particularly from the 19th century when most glaciers in the world reached a Neoglacial maximum extent (e.g. Grove, 2008). If such DEMs are available, they are usually generated from contour lines that were digitised from associated topographic maps (e.g. Paul, 2010). These maps have often limited geographic quality, inaccuracies and uncertainties (e.g. Freudiger et al., 2018; Weber et al., 2020). Historical photographs are also a good source of elevation information when properly processed (Geyman et al., 2022; Girod et al., 2018; Hannesdóttir et al., 2015; Midgley and Tonkin, 2017; Mölg and Bolch, 2017).

The methods applied so far for reconstruction of historic glacier surfaces vary between simple (e.g. Lee et al., 2021) or more complex (Glasser et al., 2011) applications within a Geographic Information System (GIS) or the use of ice flow models (e.g. Jouvet et al., 2009; Plummer and Phillips, 2003), each having specific pros and cons when working with sparse data and a highly variable sampling, possible break lines, elevation points and/or contours, topographic structures, etc. Reconstructing historic glacier surfaces using numerical glacier models (e.g. 2D flow line models) is challenging due to uncertainties in historical climate data used to reconstruct the mass balance history (Marzeion et al., 2012) and numerous glacier-specific factors such as bed topography, response times, shear stress and ice dynamics influencing glacier behaviour (Linsbauer et al., 2012; Rea and Evans, 2007).

Accordingly, simplified approaches have been developed for reconstructing past surfaces of individual glaciers. For example, Benn and Hulton (2010) introduced an Excel spreadsheet to reconstruct glacier surface profiles, whereas Khan et al. (2014) calculated point elevation changes since the LIA using the elevation change measured on the glacier margin. A similar approach has been applied by Glasser et al. (2011) and Carrivick et al. (2012) who included elevation points along the centreline to better represent surface curvature. Pellitero et al. (2016) used a combined approach of modelling and GIS to obtain the ice thickness along the centreline of paleo glaciers and hence the surface of past glacier extent. The reconstructed glacier surfaces allow to determine past glacier volume by subtracting a DEM with today's ice-free glacier bed from the DEM that refers to the reconstructed past surface. If a glacier is still present in today's DEM, volume changes can be calculated, but obtaining total volume would require a glacier bed.

Although total glacier volumes can also be estimated with simplified approaches for large samples of glaciers (e.g. Haeberli and Hoelzle 1995), reconstruction of the glacier bed requires to model the ice thickness distribution for the regions covered by glaciers. This is usually done by combining a DEM representing today's glacier surface with various auxiliary datasets such as centrelines (e.g. Linsbauer et al., 2012), approximations of mass flux (Farinotti et al., 2009) or surface flow velocities (Werder et al., 2020). Some of these approaches have been applied globally so that a modelled glacier bed (or DEM without glaciers) is available for all glaciers in the world (Farinotti et al., 2019; Millan et al., 2022). More recently, Jouvet (2022) used deep learning to model the ice thickness distribution and ice surface of past glacier extents at the same time. Although this approach can be applied at a regional scale, our focus here is on using the available input datasets (todays DEM and glacier extents plus LIA glacier extents) directly for glacier surface reconstruction with a GIS rather than fitting a model to them.

Glacier surface reconstructions using a GIS require:
(1) constraints of the outer glacier boundary,
(2) a modern DEM (e.g. to assign elevation values) and
(3) a method to create a surface between the outlines.

(1) Former glacier extents are usually marked by trimlines and / or lateral moraines. A glacier trimline separates areas affected by glacier erosion and deposition from unaffected areas and can thus be used to estimate glacier surface elevation along their boundaries (using a DEM)

during maximum extent. Lateral and terminal moraines are ridges or hills formed by the deposition of rocks and finer material carried forward on the glacier surface or its front as the ice moves. Trimlines and moraines can be recognized on aerial or satellite images, thus serving as a base for the digitising of former glacier extents (Baumann et al., 2009; Carrivick et al., 2019, 2020, 2022, 2023; Lee et al., 2021; Reinthaler and Paul, 2023; Wolken et al., 2005). However, the date of moraine deposition and maximum extent is only available from ground surveys of a few glaciers (e.g. using methods such as dendrochronology, lichenometry, surface exposure and radiocarbon dating as well as iconography) and typically averaged and assumed to be valid for a larger region. This introduces uncertainties when calculating area change rates. Additional uncertainties include (a) the digitising uncertainty, (b) the possible variable interpretation of geomorphological features by the analyst and (c) geolocation issues of the input datasets (glacier outlines and satellite images). The total uncertainty is estimated to be around 10% of the glacier area with the interpretation being the largest contributor (Reinthaler and Paul, 2023).

(2) In combination with a DEM, additional datasets supporting the spatial interpolation can be created, for example, elevation points along outlines and centrelines, elevation contours and boundaries of the ablation/accumulation area. As the ablation area is the region where most of the glacier mass loss occurs, some studies have restricted volume change calculations to this area using a proxy for the Equilibrium Line Altitude (ELA) to separate both regions (Carrivick et al., 2020, 2023; Lee et al., 2021). However, over a century timescale, there is likely also some surface lowering in the accumulation area and a method that is not considering this region will underestimate real volume loss. How large this bias is, is poorly known but estimated by Carrivick et al. (2020) to be about 20%.

(3) The methods to be used for spatial interpolation between points and/or lines of known elevation are challenged by the special geomorphometric properties of glacier surfaces, in particular their curvature. Curvature is measured in the direction of flow (profile curvature) and perpendicular to it (plan curvature). Valley glaciers tend to have a convex plan and profile curvature in the ablation area which are both getting increasingly concave towards the headwall (Benn and Evans, 2010). Thereby, the profile curvature is strongly influenced by the shape of the bedrock (i.e. concave at the headwall and below a rock ridge and convex when flowing over such a rock ridge). Whereas ice caps retain a convex plan and profile curvature also in the accumulation area (although very flat), both surface curvatures are prescribed by the shape of the bedrock for thin mountain glaciers. A simple connection of points with the same elevation from one side of the glacier to the other will thus underestimate surface elevation in regions

with a convex curvature (plan and profile) and overestimate it when curvatures are concave. A main goal of any method used for the spatial interpolation of glacier surfaces is thus to consider this variability in surface curvature, at least at a larger glacier-wide scale.

With this study we want to address the challenges described above and presented in previous work (a) by providing a yet missing in-depth analysis and intercomparison of surface interpolation methods (to determine which of them can best replicate a glacier surface), by quantifying the impact on calculated volume changes when (b) using additional data such as elevation values assigned to centreline points or (c) by considering the so-far neglected elevation changes in the accumulation region and (d) by introducing a new method of surface interpolation (upscaling approach) that retains the curvature of the glacier surface and can also be applied to ice caps and to glaciers without trimlines. To identify widely applicable methods and robust approaches, the tests and comparisons are performed in two different study regions, one with ice caps (southern Novaya Zemlya) and one with a dominance of valley and mountain glaciers (Switzerland).

2. Study regions

The two study regions are located on Novaya Zemlya in the Russian Arctic and in the Bernese Alps of Switzerland (Fig. 1). They have been selected due to the different glacier types (ice caps with and without outlet glaciers vs. classical valley and mountain glaciers), the availability of validation data and glacier outlines from different points in time being available from earlier studies.

2.1 Novaya Zemlya

The first study region includes a sample of 90 land terminating glaciers (643 km^2) in the southern part of Novaya Zemlya in the Russian Arctic, south of the Severny Ice Cap (72-74°N). The cold, high-latitude climate with numerous peaks rising above 1000 m favours significant glacier development and the presence of cold and poly-thermal ice. The glacier types are mainly ice caps with outlet valley and piedmont glaciers, some of which may be of surge-type (Grant et al., 2009). Since the end of the LIA (second half of 19th century), the 90 glaciers have split into 172 ice bodies, with a relative area loss of -26% and an increase in minimum elevation of 70±89 m (Reinthaler and Paul, 2023).

According to Zeeberg and Forman (2001), Anutsina Glacier to the north of the study area was close to its LIA maximum position in 1913. Between 1913 and 1952, tidewater glaciers in Novaya Zemlya showed the largest retreat of the 20th century (>300 m a^{-1}). From the 1960s to the 1990s, tidewater glaciers in the north of Novaya Zemlya stabilised due to years of positive mass balance related to positive North Atlantic Oscillation (NAO) phases. Between 1992 and 2010, land-terminating glaciers in northern Novaya Zemlya retreated on average 4.8 m a^{-1}, an order magnitude slower than marine-terminating glaciers (Carr et al., 2014). In the last two decades, the surface of the same sample of glaciers has lowered by about -0.8 m a^{-1}, which is much higher than the regional average (Russian Arctic) of -0.24 ± 0.03 m a^{-1} and twice the global average of -0.46 ± 0.02 m a^{-1} (Hugonnet et al., 2021).

2.2 Bernese Alps

The second study region covers 266 glaciers (today 304 entities) in the Bernese Alps in central Switzerland, an intensively studied region regarding glacier changes. The region is one of the most densely glacierized regions in the Alps with many large valley glaciers (including Great Aletsch Glacier, which is the largest one in the Alps), steep terrain and multiple peaks above 4000 m elevation. Other glacier types include small cirque and steep hanging glaciers as well as a plateau glacier (Plaine Morte).

According to Zumbühl and Nussbaumer (2018), glaciers reached their last maximum extent in the mid-19th century (1855/66 for the Lower Grindelwald Glacier), whereas some glaciers have already reached their (not much larger) LIA maximum in the 17th century. Several glaciers in the region are depicted in historic paintings (e.g. Zumbühl et al., 2016; Zumbühl and Holzhauser, 1988) and topographic maps like the Dufour Altas (mid 19th century) and Siegfried map (1882 for Aletsch glacier) have both been created close to the LIA maximum glacier extent. In Switzerland, the glacier extent was reduced by 27% between around 1850 and 1973 (Maisch et al., 2000) and by 47% until 2010 (Freudiger et al., 2018). Two of the glaciers with the longest observation periods (Lower Grindelwald and Great Aletsch) experienced surface lowerings of -0.45 m a^{-1} (1861-2012) and -0.56 m a^{-1} (1880-2017), respectively (GLAMOS, 2022). In the last two decades, glaciers in the Bernese Alps experienced a much higher surface lowering of -1.14 m a^{-1}, slightly higher than the regional average of -1.0±0.06 m a^{-1} derived by Hugonnet et al. (2021).

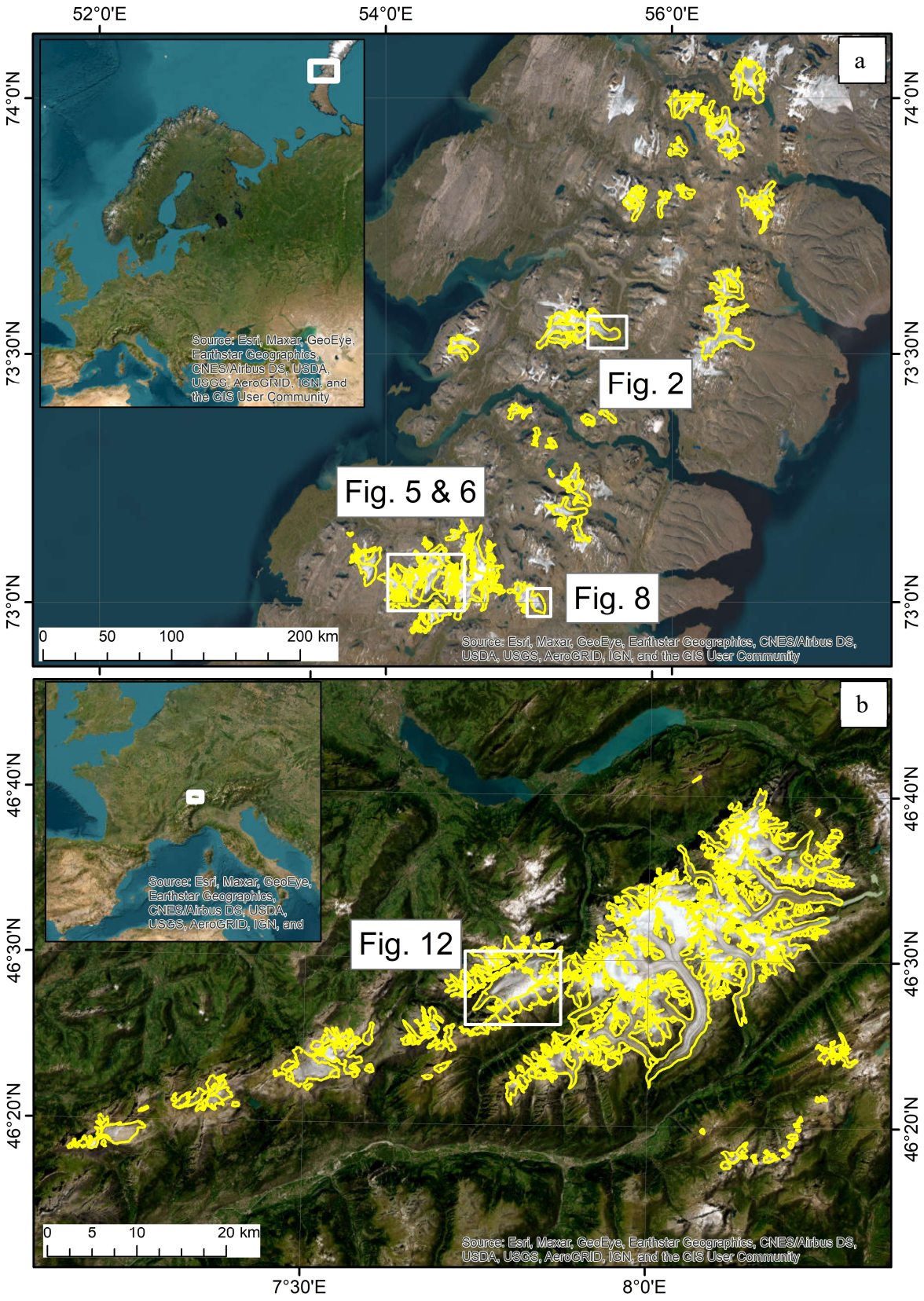

Fig. 1. The two study regions with mapped LIA glacier outlines (yellow) on a) Novaya Zemlya in Arctic Russia and b) the Bernese Alps in Switzerland. The insets show white boxes indicating where the two regions are located. Locations of some other figures are marked by white boxes in the upper panel. All background images: ESRI (2023).

3. Data

3.1 Input data

Glacier outlines from both LIA and modern times were used as an input for both regions. For Novaya Zemlya, the LIA outlines were digitised by Reinthaler and Paul (2023) with some newly adjusted drainage divides for this study, and for the Bernese Alps outlines from Maisch et al. (2000) were used. Modern outlines for 2016 are from Rastner et al. (2017) for Novaya Zemlya and from Linsbauer et al. (2021) for the Bernese Alps.

Elevation information along outline and centreline points (90 m spacing) were derived from modern high-resolution DEMs (ArcticDEM v3 for Novaya Zemlya and swissALTI3D for the Bernese Alps). After conducting tests with 45 m and 180 m point spacing, where we observed minimal differences, we selected a 90 m spacing (Fig. S6). The 45 m spacing required more computational resources, whereas a 180 m spacing reduced the accuracy especially for smaller glaciers.

Additionally, geometrically smoothed LIA glacier centrelines were created using the tools available for the Open Global Glacier Model (OGGM) by Maussion et al. (2019), which are based on the algorithm by Kienholz et al. (2014). Modern centrelines (with multiple tributaries) used for an interpolation method test were downloaded from the OGGM website (https://docs.oggm.org/en/stable/cloud.html). An overlay example of all vector input datasets is shown in Fig. 2. Further details on the input datasets are summarized in Table 1.

Table 1. Overview of the input and reference datasets used in this study.

Region	Novaya Zemlya				Bernese Alps			
Datasets	Modern		LIA		Modern		LIA	
	Name (Year, resolution)	Reference	Name (Year)	Reference	Name (Year, resolution)	Reference	Name (Year)	Reference
Outlines	Modern (2016)	(Rastner et al., 2017)	LIA (≈1850)	(Reinthaler and Paul, 2023)	Modern (2016)	(Linsbauer et al., 2021)	LIA (≈1850)	(Maisch et al., 2000)
DEM	ArcticDEM v2 (2018, 2 m)	(Porter et al., 2018)			swissALTI3D (2016, 2 m)	Swisstopo[1]	Dufour Atlas (1839-1862)	(Maisch et al., 2000; Wipf, 1999)

[1] https://www.swisstopo.admin.ch/de/geodata/height/alti3d.html

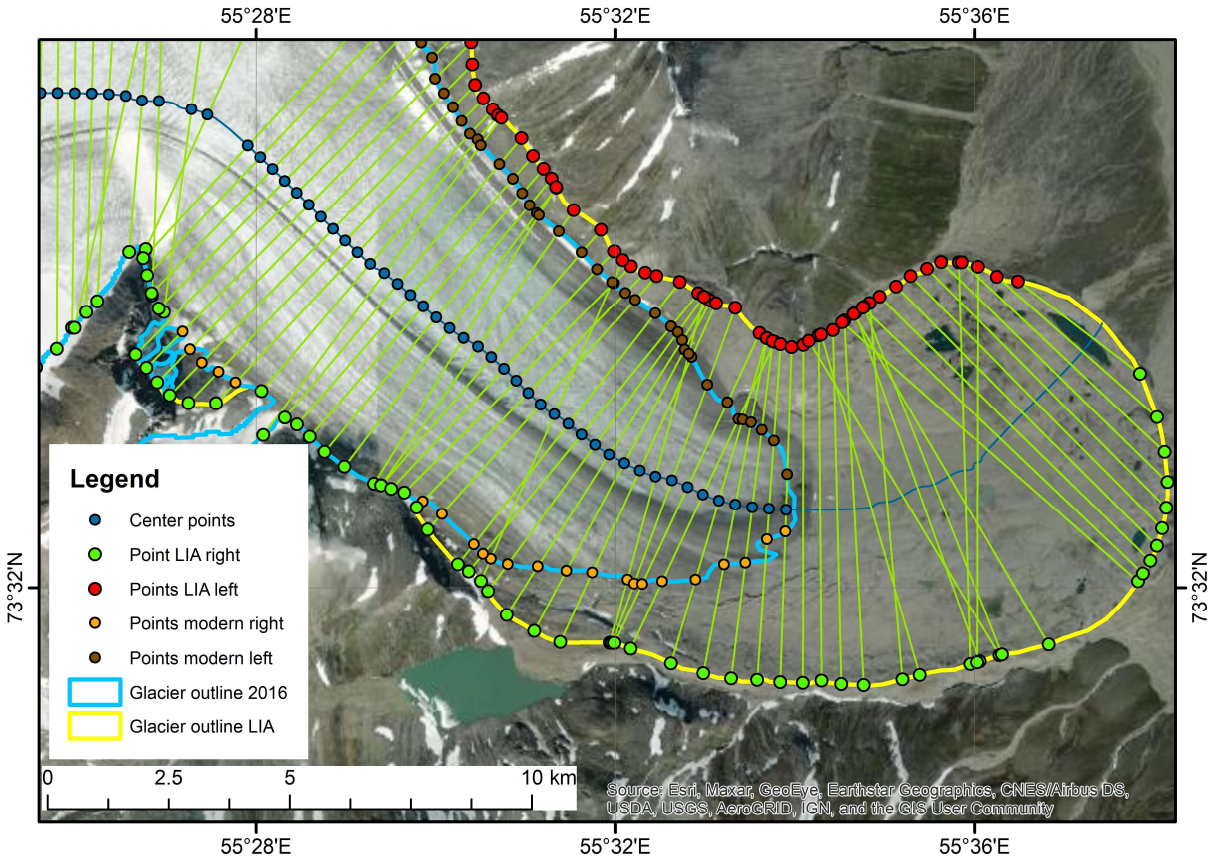

Fig. 2. Example of the LIA glacier reconstruction input data at an example glacier (RGI60-09.00254) on Novaya Zemlya. Background image: ESRI (2022).

3.2 Intercomparison data

3.2.1. Historic elevation contour lines for Switzerland

For the Bernese Alps, a reference DEM reconstructed by Paul (2010) was available for comparison. It is based on digitised elevation contour lines with 100 m equidistance from the original "Messtischblätter" digitised by Wipf (1999). They were surveyed between 1839 and 1862 at a scale of 1:50,000 and built the foundation for the Dufour Atlas (Swisstopo, 2023). Elevation contour lines for more remotely located glaciers were partly summarized and could display large errors (Maisch et al., 2000; Wipf, 1999). Additionally, digitising contributes a 5% increase in uncertainty, alongside errors resulting from geo-referencing (various distortions) as additional contributors (Freudiger et al., 2018). The historic contour lines are thus not perfect, but provide an independent validation dataset.

3.2.2. Recent elevation changes and glacier bed topography

To compare elevation changes from the LIA until today to more recent changes, the dataset provided by Hugonnet et al. (2021) was used. In their study, they generated global glacier

elevation change maps (100 m resolution) from satellite derived DEMs for 5-year periods between 2000 and 2019. The latter dataset was also used as the foundation for the up-scaling approach applied to glaciers in both regions (see Section 4.3). To relate glacier specific volume changes to the total glacier volume, ice thickness data from Millan et al. (2022) were used. This study used satellite derived flow velocities from 2017-2018 and surface DEMs to compute global ice thickness maps (50 m resolution) based on the shallow ice approximation.

4. Methods

In the following we shortly describe the here investigated methods for spatial interpolation (cf. Table 2), before we present the results of the classical methods (including our modifications) and our new up-scaling approach for reconstruction of LIA glacier surfaces (cf. Table 3).

Table 2. Overview of the interpolation methods tested for glacier surface reconstruction.

Interpolation methods	Functionality	Description	Advantage/disadvantage	Reference
Natural Neighbor (NN)	Distance weighting + area percentage	Smooth surface, no peaks pits and ridges	Works well for point data	https://desktop.arcgis.com/en/arcmap/10.3/tools/spatial-analyst-toolbox/how-natural-neighbor-works.htm
***Topo to Raster* (TtR)**	Iterative finite Difference interpolation	Designed for hydrology	Works with points and contours	https://desktop.arcgis.com/en/arcmap/10.3/tools/spatial-analyst-toolbox/how-topo-to-raster-works.htm
Inverse Distance Weighting (IDW)	Linear distance weighting	Value according to distance to other values	Simple, smooth surface	https://desktop.arcgis.com/en/arcmap/10.3/tools/spatial-analyst-toolbox/how-idw-works.htm
Kriging	Statistical analysis of data + spatial modelling	Two methods, ordinary and universal. Several semi variogram options	Limitations if points are not spatially distributed	https://desktop.arcgis.com/en/arcmap/10.3/tools/spatial-analyst-toolbox/how-Kriging-works.htm
Spline	Fits mathematical function to points	Creates minimum curvature function Two options, regular and tension (tension is better).	Creates curved surfaces	https://desktop.arcgis.com/en/arcmap/10.3/tools/spatial-analyst-toolbox/how-Spline-works.htm

4.1 Test of spatial interpolation methods using modern outlines and DEMs

Previous studies have already investigated the performance of interpolation methods for LIA glacier surface reconstruction, by testing the sensitivity of the interpolation method to volume changes (Carrivick et al., 2019; Glasser et al., 2011) and conducted tests to reproduce the moraine crest elevation (Lee et al., 2021). We here apply these methods to our study regions and add a comparison of the interpolated surfaces to a reference dataset in order to evaluate if the specific properties of a glacier surface can be reproduced. The interpolation methods (cf. Table 2) were applied to point elevations of modern outlines and the resulting glacier surfaces compared to existing modern DEMs (ArcticDEM for Novaya Zemlya and swissAlti3D for Switzerland). The tested methods include: *Natural Neighbor* (NN), *Topo to Raster* (TtR), Spline, *Kriging* and Inverse Distance Weighting (IDW). Default parameters were used unless indicated otherwise.

A smooth surface without peaks, sinks, or ridges is produced by NN interpolation using a distance weighting and area percentage-based method. This method is known to also work well with point data. *Topo to Raster* interpolation is a finite difference method used in hydrology that considers elevation values from points and contours to assign elevation values based on elevation changes (e.g. Hutchinson, 1989). Here we have used parameters optimised for point data without enforcing drainage. Since the TtR interpolation is designed to produce hydrologically correct DEMs with concave surfaces, we additionally inverted the DEM before the interpolation (i.e. the lowest point becomes the highest) to better replicate the convex surfaces of glaciers in the ablation area. The IDW interpolation creates smooth surfaces by using a linear distance weighting scheme to determine the value of a new point. Kriging, a statistical analysis and spatial modelling technique, can provide more accurate results for data with directional bias because it considers the spatial correlation between data points. Different methods (ordinary and universal) and semi-variogram models were tested. Finally, Spline interpolation creates a minimum curvature surface by fitting a mathematical function to the elevation points; here tension and regularised options were tested.

In a second round of tests, elevation values of centreline points were additionally included for the above methods and compared against the original results. The inclusion of centre point elevations promises to provide a better representation of the surface in the case of strongly concave or convex shapes, as well as unilateral glaciers (with more ice on one side). After evaluating the performance of each method by comparison with the modern DEM, the best method was selected for the LIA surface reconstruction. The relative difference to the respective modern DEMs was calculated as both glacier-specific and elevation-dependent (in 50 m

bins). All glacier surfaces produced were saved as raster GeoTIF files with a resolution of 30 m for both regions.

Table 3. Overview of methods used for glacier surface reconstruction.

	Name	Input data	Pre-processing	Additional processing steps	Interpolation method	Output (resolution)
1a	Modern glacier replication	glacier outline, DEM	convert outline to points (90 m distance), extract elevation value		Test of: TtR, Kriging, IDW, NN, Spline	Surface elevation (90 and 30 m)
1b	Modern glacier replication with centre points	Additionally, centrelines	convert outline to points (90 m), extract elevation value	Convert centreline to points (90m)	Same as 1a	Surface elevation (30 m)
2a	LIA reconstruction (classical approach)	Glacier outline, DEM	Convert outline to points (90 m distance), extract elevation value		TtR	Surface elevation (30 m)
2b	LIA reconstruction with centre points	Same as 2a, centrelines, modern outlines	Convert outline to points (90 m), extract elevation value	Create centre points with LIA elevation; more details in Supplement	TtR	Surface elevation (30 m)
3	Upscaling of Hugonnet et al. (2021)	Elevation change data 2000-2019	Create scaling factor from observed thickness changes; create elevation change gradients	Combine new LIA surface inside the recent extent with LIA outline points	TtR	Surface elevation (30 m)

4.2 GIS-based LIA surface reconstruction

Assuming that the elevation change along a glacier cross section is about uniform, one can use the elevation change (dh_m) between the modern glacier margin and lateral moraines or trimlines and transfer it to the points of the centre line (Fig. 3). This approach is based on Khan et al. (2014), who have tried this for three sample points on one glacier. We have automated the processing to have it applicable for large glacier samples. First, we have created glacier cross-sections perpendicular to the centreline with a 90 m spacing (Fig. 2). Pairs of elevation points (where LIA and modern outlines intersect the cross sections) are created along a glacier cross-section (one pair on each side) and the elevation difference (dh_m) to the modern surface is calculated (see Eq. 1 in Supplement). At the centre point, the average of the dh_m values from both sides is added to the modern DEM (Eq. 2 in Supplement). The additional information is only

valid within the margin of the modern glacier. About two-thirds (1073 out of 1511 in Novaya Zemlya) of the points are located in the ablation area. Incorrectly calculated cross sections, either parallel to the flow line or extending into a tributary glacier, were manually removed. The method promises better performance for Piedmont-type outlet glaciers with large moraine walls as well as for the accumulation area. As a note, the modern minimum elevation of glacier termini can be below those from the LIA when the terminus is now resting on the ground of the valley floor whereas it has been on the top of the moraine crest at the LIA. A detailed description of the processing steps and equations can be found in the Supplement.

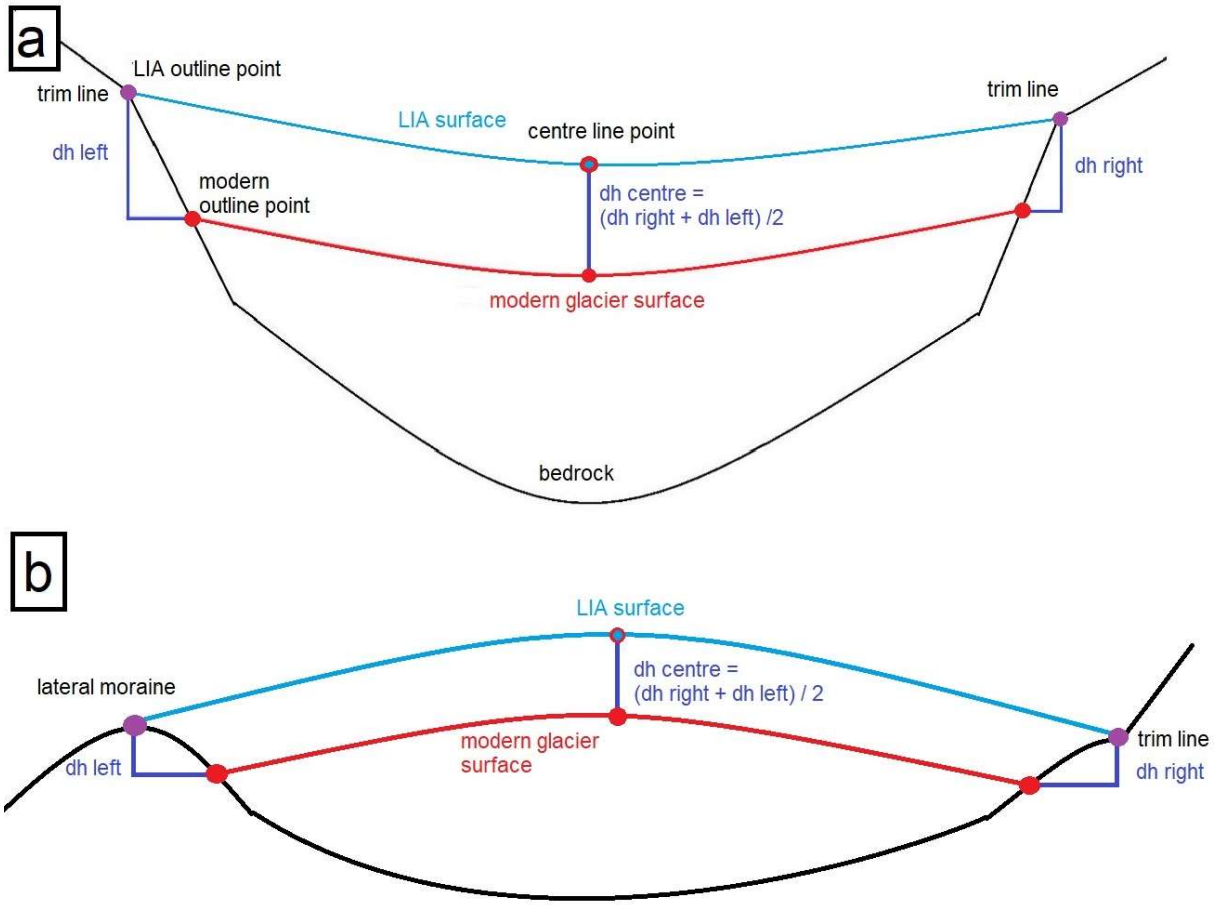

Fig. 3. Sketch of the LIA surface reconstruction method using centre points (red points) for a) the accumulation and b) the ablation area.

4.3 Up-scaling of recent elevation change data

4.3.1. Background

With glacier elevation change (dh) information being globally available from Hugonnet et al. (2021) for recent years, shifting the modern glacier surface to the LIA surface would allow to obtain a LIA surface and retain its modern spatial variability and surface morphology as well

as its curvature. The approach is similar to the delta-h method presented by Huss et al. (2010) for the determination of future glacier surface, area and volume evolution, but instead of subtracting averaged annual elevation changes until the glacier bed is reached, they are added until the LIA elevation is reached (Fig. 4). The assumption is that the elevation change gradient (its change with elevation) should not change significantly over time, similar to mass balance gradients. In other words, the pattern of elevation loss with elevation (or alternatively normalized glacier length) is assumed to be constant through time (Schwitter and Raymond, 1993).

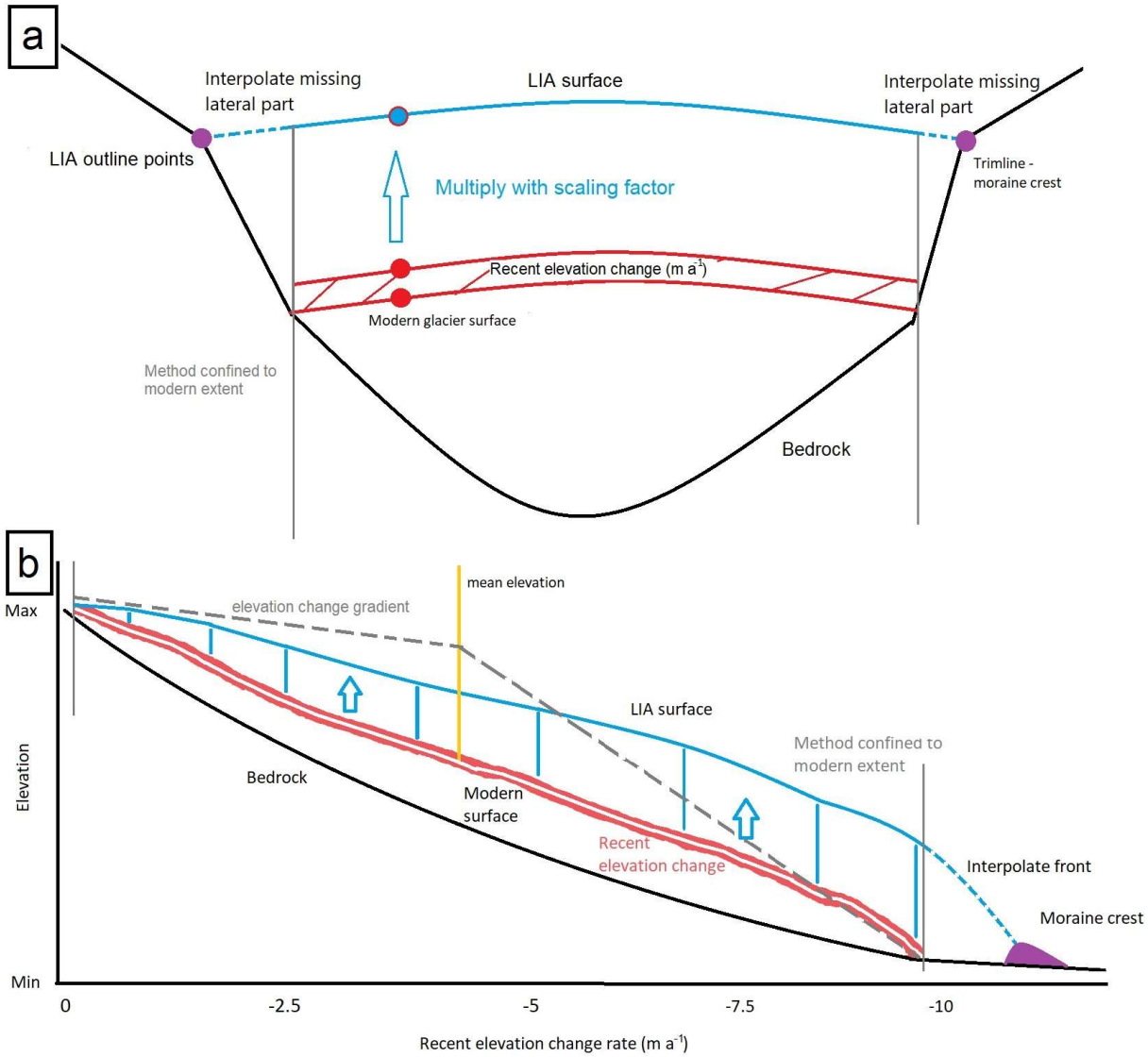

Fig. 4. Sketch explaining the up-scaling method where a) shows the cross-section of the method and b) the longitudinal profile. The modern glacier surface and the recent elevation change are marked in red, the LIA surface in blue and the LIA outline points/moraine in violet. The orange vertical line in b) marks the mean elevation where the elevation change gradient (grey dashed line) has its break point. Slope and intercept values were extracted for both gradients to predict the elevation change rate for a specific elevation. Grey vertical bars mark the confinement of the method to the modern extent, outside this area, the surface has to be interpolated. Elevation change rate values are only symbolic.

Indeed, the area between modern and LIA outlines still requires spatial interpolation when using this method, but a glacier bed is not required. Where information on elevation changes since the LIA is available (e.g. for valley glaciers with good potential GIS reconstruction using outline elevation points or historic topographic maps), it is used to determine a scaling factor from more recent change rates. This factor can then be applied to glaciers without reliable past elevation change and area change information (e.g. outlines) from geomorphological reconstruction. This is the case for most accumulation areas and ice caps. On Novaya Zemlya, we have tested various methods for glaciers with and without LIA change constraints, with a regionally averaged as well as a glacier-specific elevation change gradient.

4.3.2. Calculation of the scaling factor

Up-scaling of recent elevation changes (Fig. 5a) to reconstruct a LIA DEM requires a scaling factor. This factor was calculated by dividing the elevation changes (dh_{LIA} in m) since the LIA (from the GIS-based approach or historical maps) by the mean annual elevation change rates from Hugonnet et al. (2021) in m a^{-1} between 2000 and 2019 (dh_h). For example, if the annual change rates over the 150 years from 1850 to 2000 were the same as for the 2000-2019 period, the scaling factor would be 150 (i.e. a linear extrapolation of current rates). A scaling factor lower than this means that recent elevation change rates are higher than in the period before (e.g. by a factor of five for a scaling factor of 30). This approach was tested on a cell-by-cell basis (Fig. 5b), as a mean value over elevation bands, with its median value per glacier and as a single regional median value (further details below).

To test the robustness of a single scaling factor for the entire sample of glaciers, a sensitivity test was performed. For this, 80% of the glaciers (72 out of 90 glaciers on Novaya Zemlya) were used to calculate the scaling factor. This was then repeated five times, each time leaving a different 20% of the glaciers out. This resulted in five different scaling factors and allowed us to assess its spread and variation for different glacier samples. Cells, where the recent elevation change is larger than the change since the LIA were set to 0 as otherwise a negative scaling factor would result and thus an unrealistic lower LIA elevation compared to the modern DEM when applying it. In the first test, the recent elevation changes were regionally averaged for 50 m elevation bands for the five samples and the LIA elevation change was applied in a distributed or cell-based manner (Eq. 3 in Supplement). Secondly, the LIA changes were averaged per elevation band and the recent changes were kept cell based (Eq. 4 In Supplement).

Additionally, we have tested a glacier specific scaling factor (see Fig. S3). Finally, the cell-based calculation with both variables (dh_h & dh_{LIA}) was also tested and the median of this method was subsequently used for the reconstruction (Eq. 5 in Supplement).

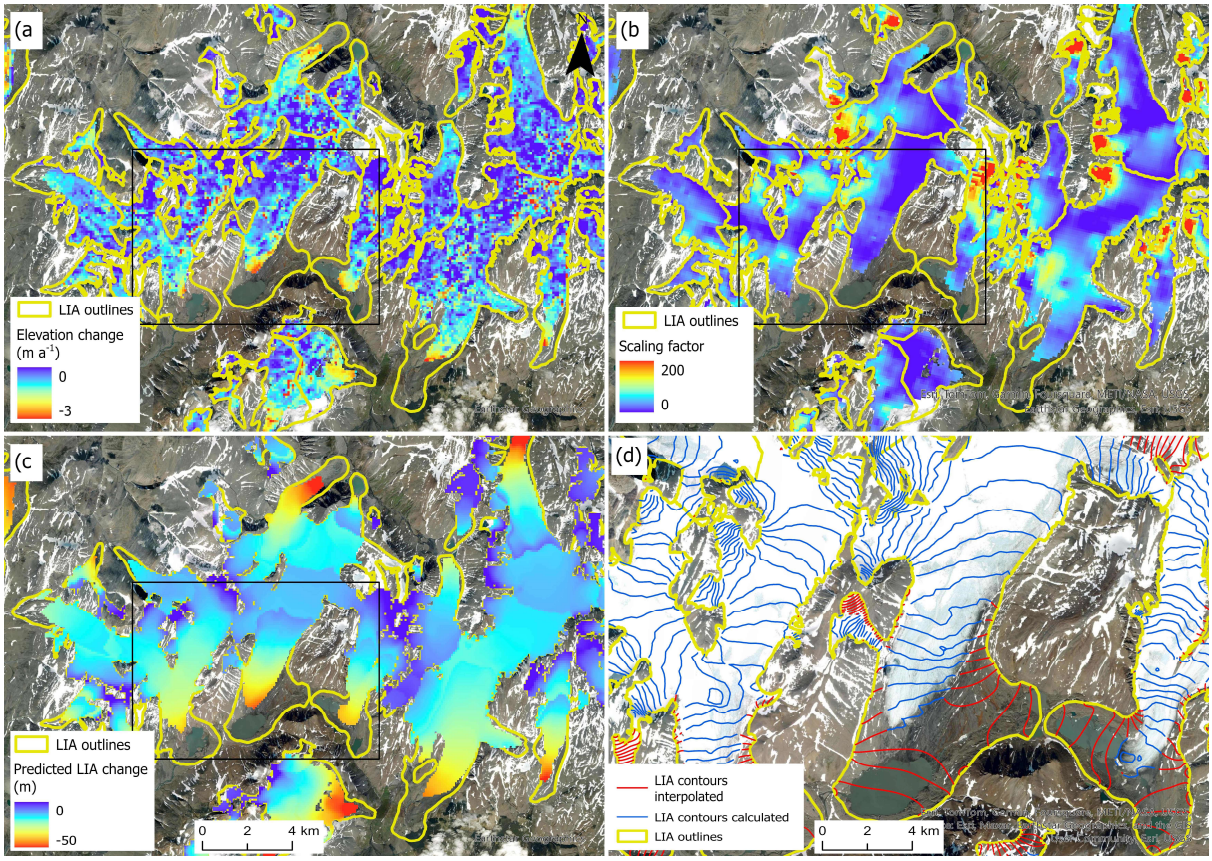

Fig. 5. Illustration of LIA surface reconstructions from scaling on Novaya Zemlya. (a) Elevation change per year between 2000 and 2020 (positive values set to zero). (b) LIA scaling factor (cell-based); (c) predicted LIA elevation changes from a dual gradient and single scaling factor; (d) generated LIA surface represented here by contour lines (blue) and interpolated contour lines outside the modern glacier extent (red). The black rectangle shows the extent of (d). All background images: (ESRI, 2023).

4.3.3. Deriving the LIA surface from glacier-specific elevation change gradients

Due to noise in the elevation change rate dataset from Hugonnet et al. (2021) and its amplification when applying the scaling factor (visualized in Fig. S7), we explored the use of a glacier-specific elevation change rate gradient. It is the relationship between the elevation change rate from Hugonnet et al. (2021) and the elevation change for each glacier individually. We have used a bi-linear regression, the mean elevation of the glacier being the breakpoint (Fig. 4b). This helped to better represent the non-linearity of elevation changes without using more complex functions. Examples of scatter plots for both regions with bi-linear gradients are shown in Fig. S2. The slope (a) and intercept (b) terms were extracted for both linear regression lines for

each glacier and together with the modern DEM an elevation change for the specific elevation and glacier predicted (Eq. 6 in Supplement).

The total elevation change since the LIA is calculated by multiplying the regressed elevation change by the scaling factor (Fig. 5c). By adding the change to the modern DEM, the LIA surface elevation was computed within the modern glacier extent (Eq. 7). To get the surface for the full coverage of the LIA extent, it was combined with the outline point elevations and interpolated (using *Topo to Raster*) over the missing area (Fig. 5d). A detailed description of the processing steps and list of equations can be found in Section 2 of the Supplement.

4.4 Calculation of a proxy for the Equilibrium Line Altitude (ELA)

To test the influence of the inclusion of the accumulation area in the volume change assessment, a proxy representing the balanced-budget ELA_0 (mean mass balance of zero) is required. As the ELA_0 is only available from time series of direct measurements, we have used the area-weighted mean elevation for each modern glacier (Kurowski, 1891). Studies have shown that this is a good approximation when working with glacier inventory data (Braithwaite, 2015; Braithwaite and Raper, 2009; Raper and Braithwaite, 2009). For the volume change assessment, we have for each glacier only considered the area below this elevation. It has to be noted that these are only generalised ELAs to divide all glaciers into two parts rather than the ELA_0 related to a zero mass balance of a specific glacier. Hanging glaciers, for example, are still divided into two parts, even though the ablation area might only be the calving front. Furthermore, the ELA_0 can vary greatly from glacier to glacier due to local conditions such as glacier hypsometry, possible debris cover, precipitation, topographic shading and exposition.

5. Results

5.1 Methods used for spatial interpolation of modern glacier surfaces

Before the statistical analysis, the different settings available for the different interpolation methods were tested. For Spline interpolation, tension seemed to perform better than the regularized type and therefore the latter was not analysed further. Similarly, for Kriging the ordinary method with a spherical semi-variogram model performed best and the other settings were not further evaluated. The visual inspection of the results (Fig. 6) also shows a directional bias, especially for Kriging and IDW where the surface is more positive and the opposite side

negative. The Spline interpolation also results in oscillating patches of positive and negative values which are not visible when looking only at the mean values. The related difference images in Figs. 6a and 6d reveal the deviations among the compared methods. Boxplots of mean values and standard deviations (STD) for each interpolation method are displayed in Fig. S1. After the visual interpretation and evaluation of the mean differences, the best methods were used for the LIA interpolation described in Section 5.2.

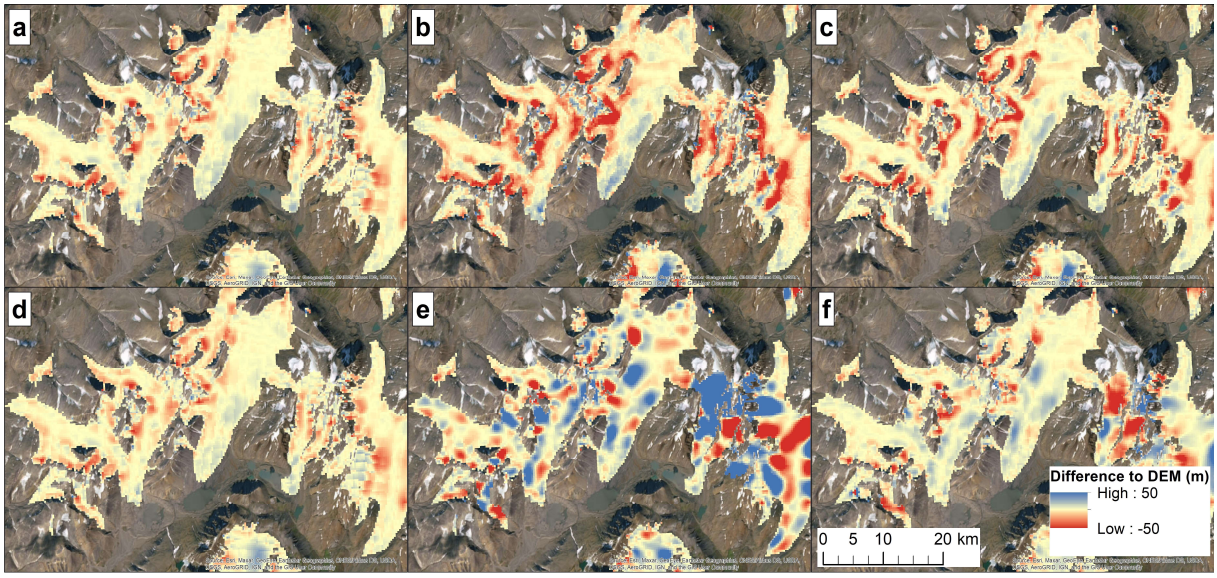

Fig. 6. Differences between interpolated surfaces (including centre points) and the reference DEM for a glacier sample in Novaya Zemlya. Interpolation methods: (a) TtR, (b) *Kriging*, (c) IDW, (d) NN, (e) *Spline* and (f) *Spline* with tension. All background images: ESRI (2022).

On Novaya Zemlya, the interpolation methods TtR and NN perform best with a mean difference of -6.76 ±16.5 m and -8.26 ±15.9 m, respectively, or-3.0 ±10.1 m and -3.4 ±10.1 m when including centre points (results for all tested interpolation methods including the coefficient of determination (R^2) and Root Mean Square Error (RMSE) values are summarized in Table 4). For the Bernese Alps, the same two methods revealed the smallest differences of -13.5 ±42.7 m and -13.9 ±71.9 m, respectively, or 7.5 ±35.5 m and -7.3 ±68.7 m when including centre points.

The two interpolation methods also show an elevation-dependent bias. In Novaya Zemlya (Fig. 7a), TtR underestimates the elevation until around 450 m a.s.l. and overestimates it in the accumulation area when using the outline points only. This is probably due to the tendency to create surfaces with a concave curvature, as its main usage is the creation of hydrologically correct DEMs. When inverting the DEM before the TrR interpolation, the difference in the ablation area decreased substantially (mean difference <5 m), whereas it increased at elevations above 500 m. On the other hand, the NN interpolation performs well in the lower area but

overestimates values between 400 m and 1000 m with a peak around 600 m (-14.4 m). This directly correlates to the elevation histogram, as most of the area is located around 600 m and thus spaces between outlines are larger. Therefore, NN fails to reproduce the concave shape of wide plateaus in the accumulation area. For the Bernese Alps (Fig. 7b) both TtR and NN performed very well (mean difference <10 m) at elevations lower than 2500 m, TtR until 2700 m. In contrast, TtR and NN have their worst performance (>25 m) at elevations around 3300 m. Generally, both methods (TtR and NN) tend to overestimate the elevation, especially at higher elevations, whereas Spline interpolation underestimated surface elevation here.

Table 4. Mean difference, standard deviation (STD), R^2 and RMSE of interpolated surfaces to the modern DEM for the different interpolation methods with and without center points (NZ = Novaya Zemlya, BA = Bernese Alps). Negative values indicate that the interpolated surface is higher than the DEM.

Interpolation method	with centre points				outline only			
	Mean difference (m)	STD	R^2	RMSE (m)	Mean difference (m)	STD	R^2	RMSE (m)
Region	NZ/BA	NZ/BA	NZ/BA	NZ/BA	NZ/BA	NZ/BA	NZ/BA	NZ/BA
NN	-3.39/-7.31	10.13/68.66	0.996/0.97	10.9/69.6	-8.26/-13.86	15.89/71.90	0.991/0.967	18.1/73.8
TtR	-2.99/-7.46	10.11/35.53	0.996/0.993	10.8/34.7	-6.76/-13.48	16.48/42.68	0.991/0.99	18.1/43.5
Spline	1.42/2.50	21.12/75.52	0.984/0.963	21.2/76.1	12.20/20.50	40.20/91.95	0.945/0.948	42/95
Kriging	-6.95/-13.43	18.20/49.36	0.988/0.986	19.7/49.7	-14.05/-27.54	27.11/64.95	0.976/0.975	30.8/69.8
IDW	-5.58/-11.26	15.33/65.80	0.992/0.973	16.6/67.2	-12.62/-24.06	24.90/76.99	0.98/0.964	28.2/81.3
TtR invert	-4.06/	10.37/	0.996/	10.8/	-8.50/	17.36/	0.991/	19.0/

Including centre points in the surface interpolation results, as expected, in smaller differences to the reference DEM. Nevertheless, the most promising methods (TtR and NN) slightly overestimate glacier elevation and thus the volume where the glaciers are widest (≈400-800 m on Novaya Zemlya and between 2500 and 3500 m in Switzerland). Inverting the DEM for the TtR interpolation did not change the result substantially, because centre points already predefine the plan curvature of the surface.

Spline interpolation is a particular case as it shows the lowest overall difference in both regions (1.4 m and 2.5 m) but a much larger variability (STD = 21.1 and 75.5 m) and thus resulting in unrealistic surfaces with alternating patches of low and high values. It is also the only method in both test regions that generated lower elevation values than the reference DEM, even when

including centre points (blue regions in Fig. 6e and 6f). On the other hand, all other methods overestimated surface elevation (more red than blue regions in Figs. 6a, 6b, 6c, 6d). Overall, Spline interpolation gave the most unrealistic results (especially without centre points) due to its polynomial curves which are problematic for replicating flat glacier surfaces.

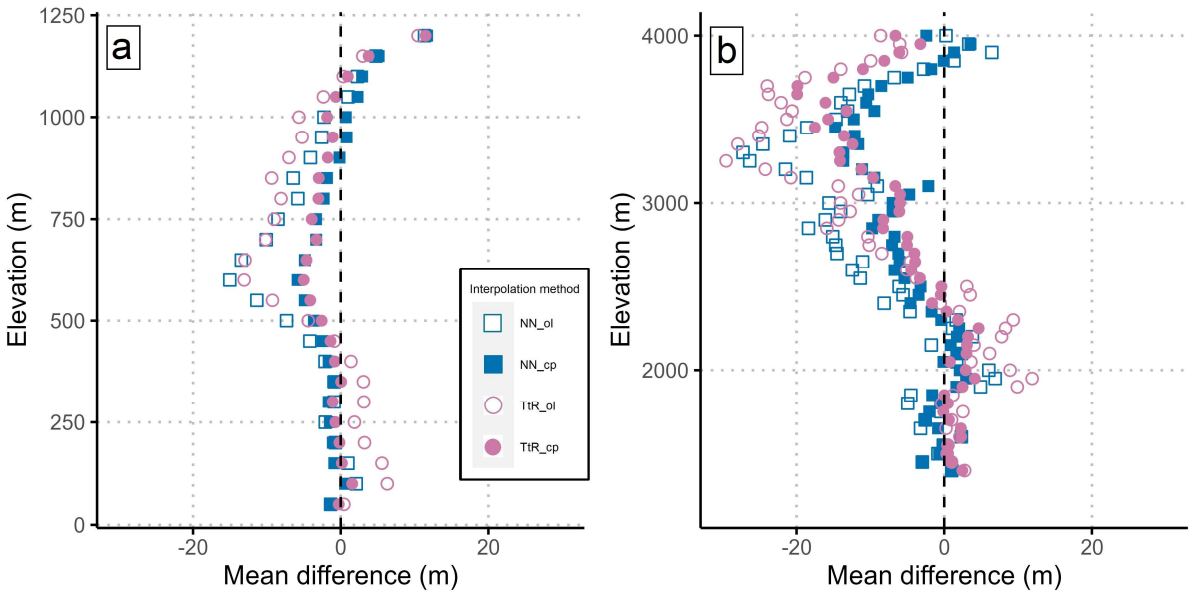

Fig. 7. Mean difference to the reference DEM vs. surface elevation for Natural Neighbor (NN) and Topo to Raster (TtR) interpolation methods with centre points (cp) and outlines only (ol). a) for Novaya Zemlya and b) for the Bernese Alps.

5.2 LIA surface reconstruction

5.2.1. GIS-based LIA surface reconstruction

For Novaya Zemlya, a total of 28,915 elevation points were used to interpolate the LIA surfaces for the 90 glaciers. Of these, 1511 points were centre points, storing information about the averaged elevation change from both glacier margins. As shown in Section 5.1, each of the interpolation methods tested yields different surface elevation values. For the reconstruction of the LIA surface, we decided to use the TtR interpolation because of its good performance in the replication test and in producing both convex (with centre points in the ablation area) and concave (accumulation area) surfaces. *Natural Neighbor* interpolation can be recommended due to its simplicity, consistency, the low mean difference in the replication test (although slightly higher than TtR) and lower spread of values compared to TtR.

The inclusion of centre points in the processing chain did not significantly change the overall result as the mean elevation change is only 1.03 m higher when using centre points. If only the

ablation area is considered, the difference increases to 1.52 m. This makes sense, as especially in shallow outlet glaciers without prominent moraines, elevation information from the centre contributes to the error reduction (see the example from Novaya Zemlya in Fig. 8). The smaller difference in the accumulation area can be explained by the lack of centre points in many areas because no trim lines were mapped.

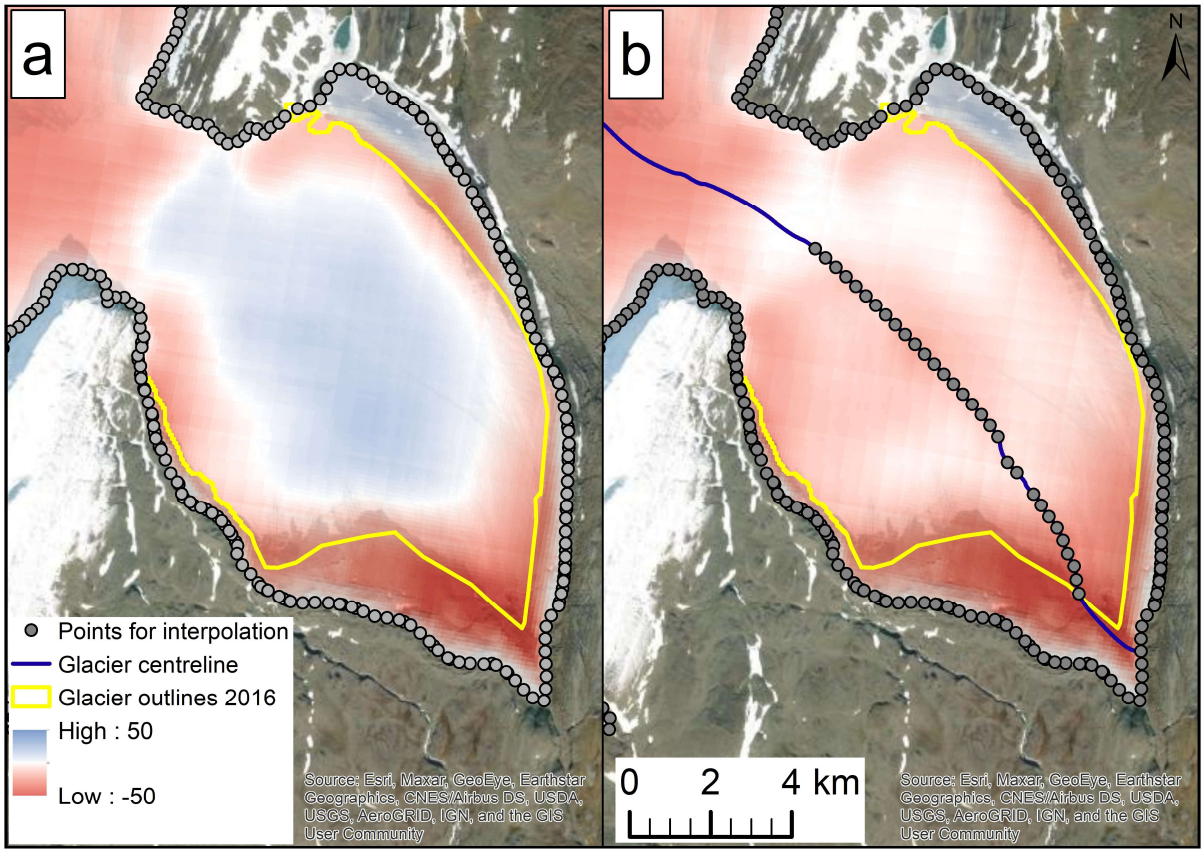

Fig. 8. Elevation change results (m) for reconstructions a) without and b) with centre points for a glacier tongue in Novaya Zemlya. The former shows an unrealistic increase in elevation in the centre of the glacier. All background images: ESRI (2022).

For the test region in Switzerland, both methods with and without centre points were tested against elevation values from the Dufour Atlas. For the interpolation, more than 24,000 outline points and an additional 531 centre line points were used. Over the entire area of 524.4 km^2, both methods have very similar mean differences with -3.7±38 m and -3.5±40 m, respectively. The median values are 2.5 m with centre points and 3.5 m when only using the outlines. The R-squared (R^2) values are 0.992 and 0.992 while the RMSE values are 38.5 and 39.8 m, respectively (Figs. S5a and S5b).

A general bias could not be detected, but an elevation-dependent bias is present (Fig. 9). Whereas the GIS-based methods underestimate the elevation below 2500 m, they overestimate them for the areas above. The lower mean value compared to the median is also reflected in the histogram which is slightly skewed due to regions with very negative values (<-200 m) in higher elevation zones (e.g. over Ewigschneefeld).

Overall, both GIS-based methods with and without centre points are suited for LIA surface reconstruction. Centre points do not lower the overall error, because for relatively small valley glaciers the space between the outline points is not large enough to get a real advantage from the centre points. Moreover, the curvature over small glaciers is of limited relevance for LIA surface reconstruction. However, for individual glaciers, the appearance of the surface DEM is more realistic when including centre points.

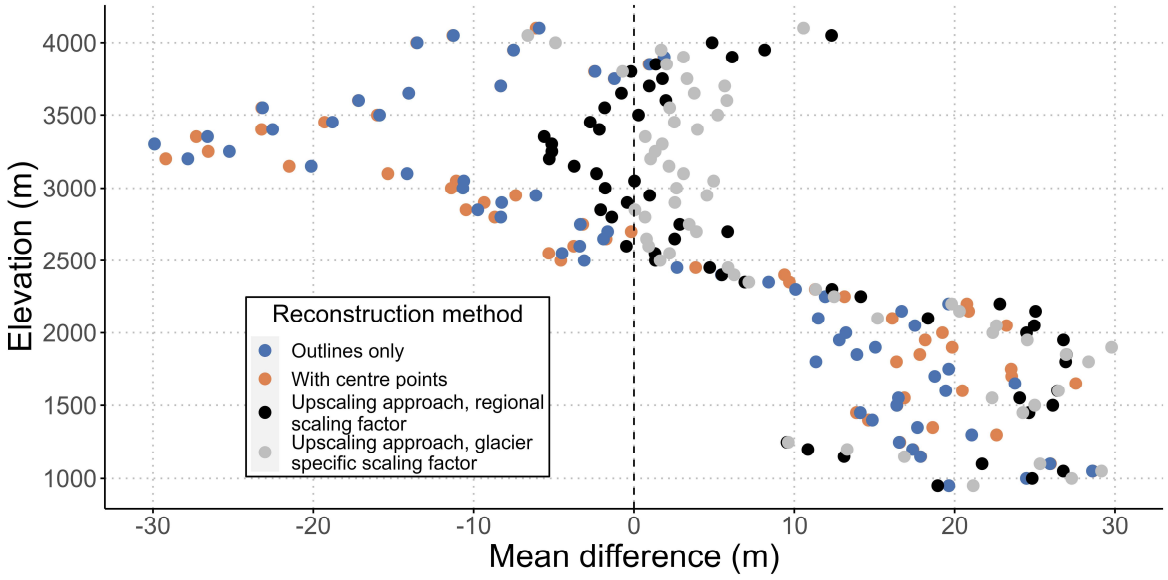

Fig. 9. Glacier elevation vs. mean difference to elevation values of the Dufour Map. Positive values indicate the Dufour map values being higher.

5.2.2. Up-scaling of recent elevation change data

In the first test, the mean elevation change per elevation band (dh_h mean elevation) extracted from the Hugonnet et al. (2021) dataset was used to explore and investigate the LIA up-scaling calibration, i.e. shifting modern glacier surfaces to their LIA elevation. The method was tested for its robustness by changing the glacier sample from which the shift was derived (Fig. 10a). The modern elevation change values for Novaya Zemlya show only limited variation (especially at higher elevations), which means that regional average elevation changes are similar

for the same elevations across glaciers and a larger spread is expected at lower elevations (maximum at 200-250 m with a STD of 0.075 m a^{-1}). In the second test, the robustness of the LIA elevation changes as input to determine the scaling factor was also tested using the same five calibration samples (Fig. 10b). The results show a larger spread at lower elevations (STD of 10.5 m) that is only reached by a few glaciers and the spread is decreasing towards higher elevations.

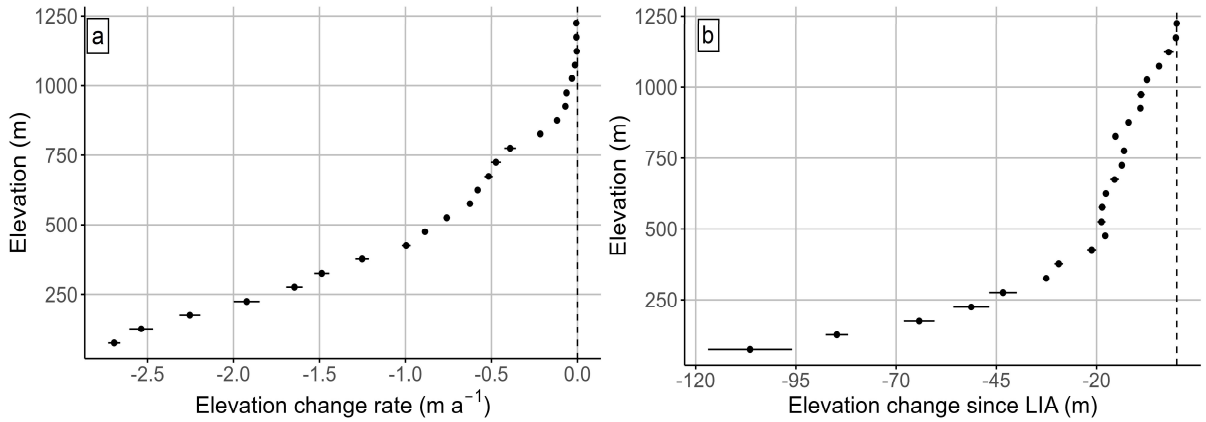

Fig. 10. a) Elevation change per year between 2000 and 2019 from Hugonnet et al. (2021). b) Elevation changes since the LIA on Novaya Zemlya. Error bars indicate the standard deviation between the different sample selections.

The calculated median scaling factors (LIA dh_{factor}) resulting from the five different outputs (for both methods, elevation band means from Hugonnet et al. (2021) and elevation band means from the LIA elevation change) are on Novaya Zemlya between 20 and 40 at lower elevations (until around 800 m), but are strongly increasing and more variable towards higher elevations (Fig. 11). This is because only a few glaciers are reaching these elevations and because the values for dh_h and dh_{LIA} are close to 0 at high elevations, resulting in a multiplication factor that can get very high while absolute changes remain low. For the Bernese Alps, the median scaling factors are also rather stable with elevation. Nevertheless, cells with a very low change in the last 20 years (possibly outside the current glacier boundary) but a large change since the LIA, result in very large values of the scaling factor, resulting in mean values being much larger than the median.

Since the scaling factor is about constant with elevation for the majority of the glacier coverage, using a single value was also tested. For this, the regional median value of the distributed dh_h and dh_{LIA} (not regional averages per elevation band) was selected and resulted in a scaling factor of 25.5 ±24.2 for Novaya Zemlya (the number excludes negative scaling values where the

recent change was higher than the change since the LIA, ± indicating the mean absolute deviation (MAD)). For the Bernese Alps, the regional median scaling factor used for the up-scaling approach is 36.1±21.3. Histograms of the scaling factor for both regions are displayed in Fig. S4.

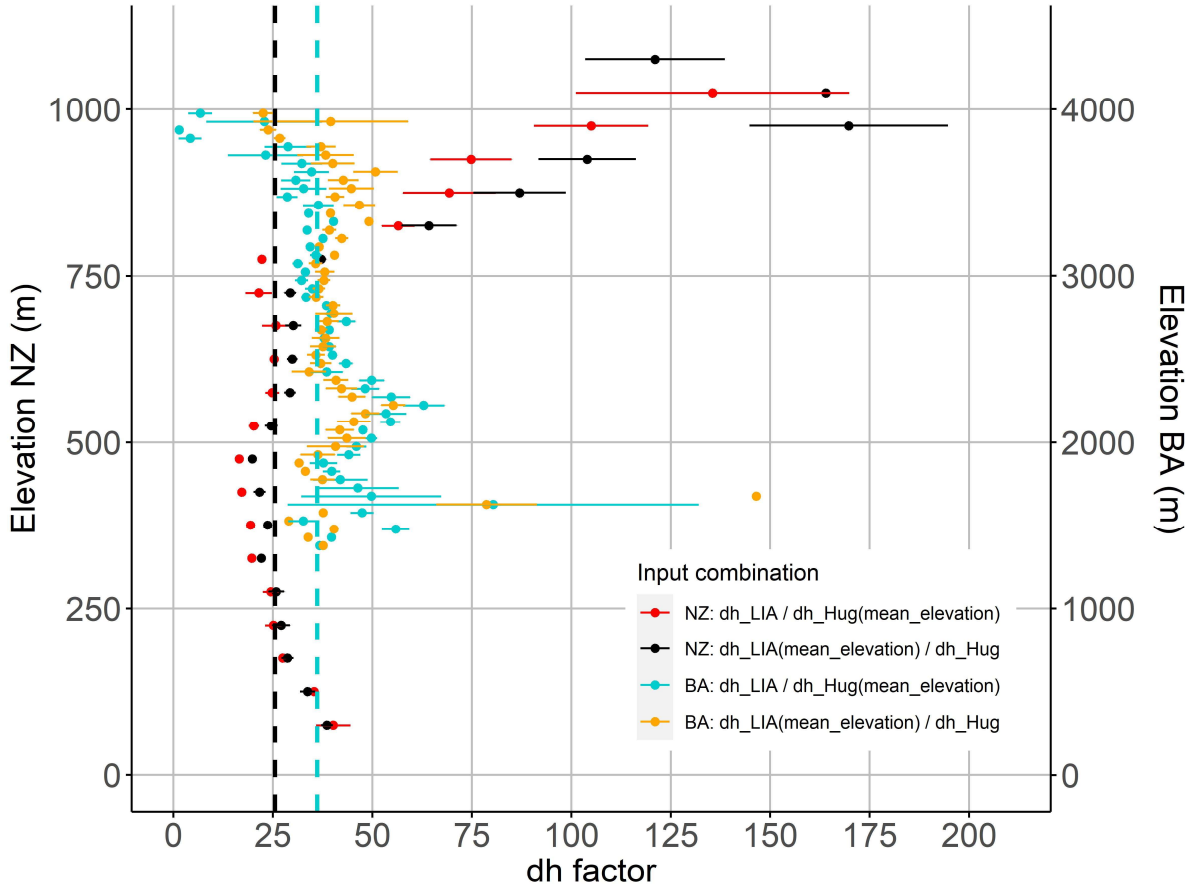

Fig. 11. Median LIA scaling factor (LIA dh_{factor}) for Novaya Zemlya (NZ) and Bernese Alps (BA) calibrated with elevation band means from Hugonnet et al. (2021) in red/blue and elevation band means from the LIA elevation change (black/orange) against the elevation. Dashed lines (black for NZ; blue for BA) indicate the cell-based median value for the entire region. Error bars indicate the standard deviation of the five different calibration runs.

A glacier specific scaling factor was also investigated, a related histogram can be found in Fig. S3 for both regions. Whereas values are in the same order of magnitude as the regional scaling factor (median of 22.3±30.3 for Novaya Zemlya and 44.0±1115 for the Bernese Alps), some glaciers especially in the Bernese Alps show very large values (> 1 million) resulting from very low dh_h values and very large dh_{LIA} values. These glaciers are all smaller than 0.05 km^2 and thus only composed of five or less pixels in the dh_h dataset. Using a regional scaling factor avoids such outliers thus this approach has been used in this study.

As explained in the methods section, a bi-linear regression of elevation change (with the mean elevation as a breaking point) was calculated for each glacier (see examples in Fig. S2). This allowed for preserving glacier-specific properties, but also led to the topographic pattern of the modern snout still being visible on the reconstructed surface. This could partly be removed by smoothing the data but has not been applied for the dataset presented here. It was also tried to predict elevation changes for the area between the modern and the LIA outline. Although it worked, it shifted the valley walls and created unrealistic results, i.e. it was also not implemented.

Comparing the reconstructed surface from the up-scaling approach (using glacier-specific elevation change gradients) with the surface using the GIS method with centre points on Novaya Zemlya, results in a mean difference of only 2.8±17 m (the latter being lower). For the Bernese Alps, the mean difference was 8.5±35.6 m. The relatively small overall differences to the GIS method can be explained by the fact that the same outline elevation points were used (but without elevation information along the drainage divide). While the surfaces in the ablation area are very similar, the up-scaling approach results in lower elevations in the accumulation area in both regions (Figs. 9, 13c and 13d). This is due to the fact that concave areas are not being filled up as in the GIS-based reconstruction. The mean difference against the reference DEM (Dufour Atlas) is 4.6±26.7 m (R^2= 0.996; RMSE = 26.7 m; Fig. S5c). When using a glacier specific scaling factor, the mean difference could not be reduced, but the spread was a bit smaller (mean difference of 6.5±23.8, R^2= 0.997; RMSE = 24.6 m; Fig. S5d). Furthermore, a glacier specific scaling factor is not applicable for glaciers where it is not possible to obtain dh_{LIA} and effects on the volume change are minimal (see details in Section 5.3.2), therefore a regional scaling factor was applied for the created dataset.
For individual glaciers, however, strong improvements were observed when using the up-scaling approach, even with a regional scaling factor as Fig. 12c for the Kanderfirn in Switzerland reveals. Only the up-scaling approach creates a realistic surface in a region where a strong change in slope (here concave profile curvature) occurs.

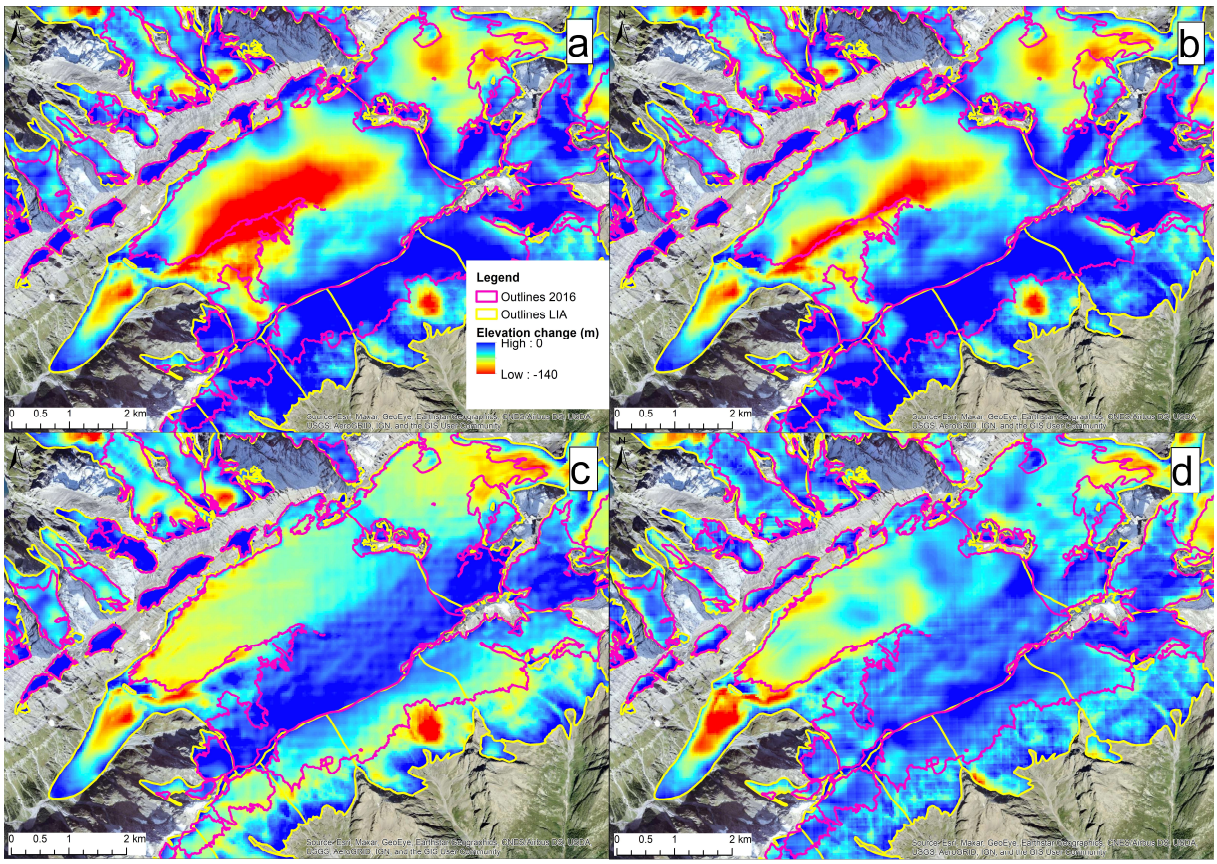

Fig. 12. Elevation changes on Kanderfirn (BA) from reconstructions using a) only outline points, b) including centre points, c) the up-scaling approach and d) the reference dataset (Dufour Atlas). All background images: ESRI (2023).

5.3 Elevation and volume change

5.3.1. Elevation changes since the LIA

The elevation change results in Table 5 reveal significant glacier thinning since the LIA maximum. Considering the entire glacier area, the reconstruction with centre points for Novaya Zemlya resulted in a mean total elevation change of -22.5 m for the reconstruction with centre points and -21.1 m for the up-scaling approach (-0.13 m a^{-1}, largely independent of the reconstruction method). The glacier-specific elevation change was on average -20.0±7.9 m and -16.6±8.4 m for the two methods, respectively. Small glaciers have generally a lower mean change than larger glaciers. As most of the glacier melt is occurring in the ablation area, also the mean elevation change values are larger when only looking at the ablation area. When using the reconstruction with centre points and outlines only, the change is around -25 m and thus roughly 15% larger than for the entire glacier area (for the up-scaling approach it is -26.8 m or 26.7% larger). The largest value (-41 m) is measured at an elevation of around 200 m for all methods (Fig. 13a) and constantly decreasing until around 500-600 m (which is approximately

the ELA). The up-scaling approach shows generally a lower elevation change in the accumulation area (10 m less at an elevation of 1000 m).

Table 5. Elevation and volume change results since the LIA using only the outlines points, including centre points and the up-scaling approach.

Region	Novaya Zemlya				Bernese Alps					
Interpolation method	*Topo to Raster*		Up-scaling approach		*Topo to Raster*		Up-scaling approach		Reference dataset	
Area of interest	Ablation area only	Entire glacier	Ablation area only	Entire glacier	Ablation area only	Entire glacier	Ablation area only	Entire glacier	Ablation area only	Entire glacier
Volume change (km^3) (outlines only)	-8.40	-13.56	-9.10	-14.59	-16.62	-27.13	-16.44	-22.7	-18.11	-25.11
Volume change (km^3) (with centre points)	-9.23	-14.21			-17.01	-27.24				
Elevation change (m) (outlines only)	-24.15	-21.49	-26.77	-21.12	-60.86	-36.42	-59.72	-30.0	-65.24	-33.27
Elevation change (m) (with centre points)	-26.45	-22.51			-62.11	-36.56				

In the Bernese Alps, glaciers experience a higher thinning compared to Novaya Zemlya. The mean elevation change from the reconstructed surface (TtR with centre points) was -36.6 m (-0.22 m a^{-1}). The mean elevation change using the reference DEM (from contour lines of the Dufour Atlas) was -33.3 m (-0.20 m a^{-1}). The lower values mostly resulted from lower changes in the accumulation area, pointing to a possible overestimation of the GIS-based reconstruction (Fig. 13b). The up-scaling approach resulted in values close to those of the reference DEM (-30.0 m, -0.18 m a^{-1}). When only considering the ablation area, the mean change from the GIS reconstruction (with centre points) was -62.1 m (-0.37 m a^{-1}) and -59.7 m (-0.36 m a^{-1}) for the up-scaling approach, thus two times higher compared to the entire glacier.

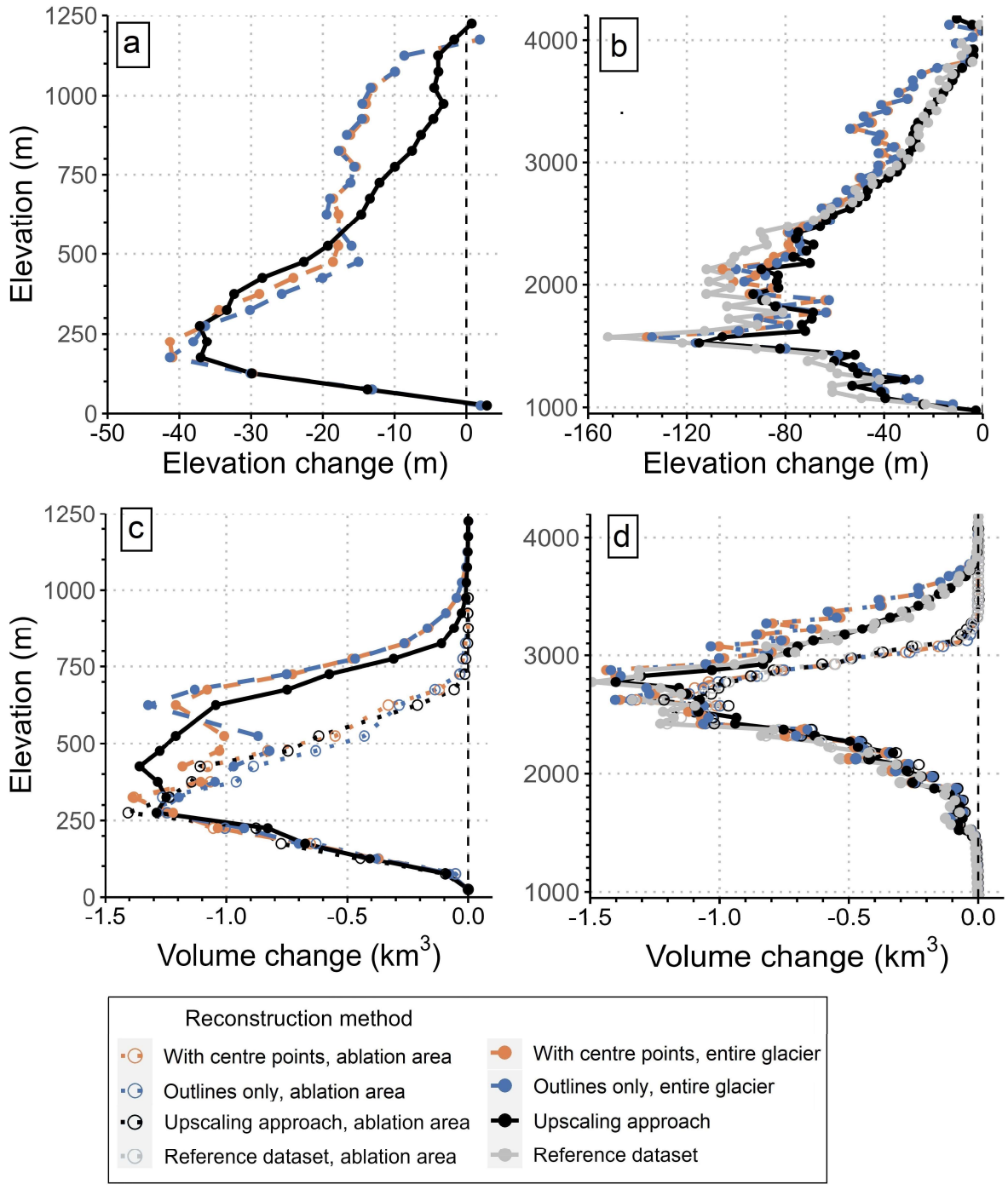

Fig. 13. Mean elevation change (panels a & b) and volume change (panels c & d) per 50 m elevation band for Novaya Zemlya (panels a & c) and the Bernese Alps (panels b & d) for all applied methods.

5.3.2. Volume change since the LIA

The modern glacier volume of the glacier sample in Novaya Zemlya is approximately 69 km^3 according to the dataset by Millan et al. (2022). The calculated volume change using the surface reconstruction shows a volume change of -14.21 km^3 for the interpolation with centre points and -14.59 km^3 for the up-scaling approach. This would result in a relative volume loss of around 17% since the LIA, regardless of the reconstruction method. The volume change per elevation band (Fig. 13c and 13d) shows the largest volume loss at elevations between 250 and

700 m. The volume loss for the ablation area is much smaller, 9.1 km^3 for the reconstruction with centre points and 9.2 km^3 with the upscaling approach. Neglecting the volume changes in the accumulation area would thus result in an underestimation of 54%.

In the Bernese Alps, the modern glacier volume is around 33.6 km^3 when using the dataset from Millan et al. (2022). The LIA volume is estimated as 60.8 km^3 so that 27.24 km^3 (or 44.8%) of ice was lost. Using the up-scaling approach with a regional scaling factor, the numbers are 56.1 km^3 for the total LIA volume and -22.7 km^3 (-40.3%) for the volume change. When using a glacier specific scaling factor, the volume change is with -22.5 km^3 nearly identical. The elevations with the largest volume losses are between 2500 and 3000 m (Figs. 13c and 13d), around the location of the mean elevation. When only considering volume changes in the ablation area, the change is -16.4 km^3 when using the up-scaling approach (27% less compared to the entire glacier).

5.4 Change of topographic parameters

Due to glacier retreat and surface lowering since the LIA, also the topographic parameters of the glaciers change. In Fig. 14 the change in the elevation profile (hypsometry) is shown. Apart from a decrease in area in all elevation bands (decreasing towards higher elevations), the overall shape of the elevation profile did not change for Novaya Zemlya but for the Bernese Alps, the peak shifted from 2850 m during the LIA to 3100 m in 2016.

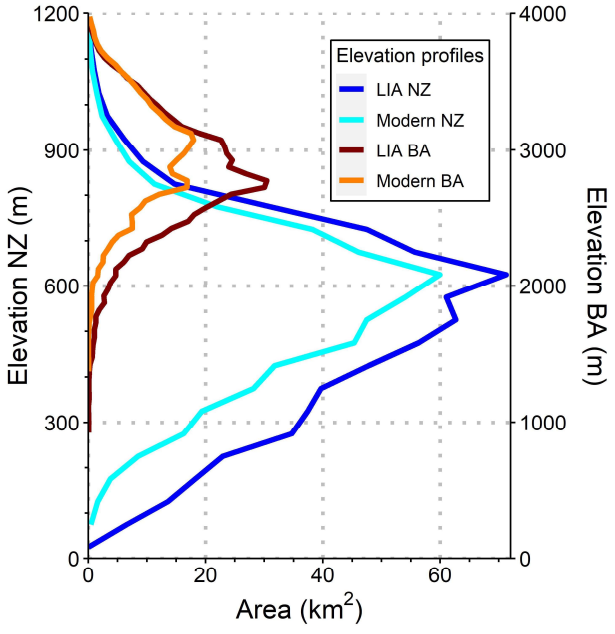

Fig. 14. LIA and modern elevation profiles (hypsometry) for both regions. The elevation for Novaya Zemlya (NZ) is displayed on the left axis and the Bernese Alps (BA) on the right axis.

Changes in mean and median elevation have more than doubled in the Bernese Alps compared to Novaya Zemlya. Only a few glaciers showed a decrease in mean elevation. This is not due to elevation gain, but results from a loss of larger parts of the accumulation area. Similarly, only a few glaciers did not experience an increase in minimum elevation or even showed a decrease. This is generally due to the LIA minimum elevation being measured on a moraine crest whereas today the terminus is located in a depression behind the moraine. An overview of the change in topographic parameters is given in Table 6.

Table 6. Topographic parameters for both regions (first value for Novaya Zemlya, second value for the Bernese Alps) and their changes (Δ) between the two periods.

	Min elev. (m)	Max elev. (m)	Mean elev. (m)	Δ Mean elev. (m)	Median elev. (m)	Δ Median elev. (m)
Modern	54/1257	1262/4190	564/2963		573/2978	
LIA with centre points	41/977	1278/4171	524/2873	40/90	535/2874	38/104
LIA up-scaling	38/977	1258/4150	521/2865	43/98	535/2866	38/112

6. Discussion

Table 7 summarizes the main conclusions for the different glacier surface reconstruction and interpolation methods. Further details are provided in the following sections.

Table 7. Usage and recommendations for the different reconstruction methods

Methods	Interpolation of outline points	Including centre points	Up-scaling of elev. change data
Recommended interpolation method	*Natural Neighbor*	*Topo to Raster*	*Topo to Raster*
Advantages	Simple, fast, widely applicable	Improving wide and piedmont glaciers	Applicable on ice caps and good performance in accumulation area; glacier specific calibration; retains surface morphology
Disadvantages	Poor performance for piedmont glaciers, ice caps and over wide glacier plateaus.	Misclassified points can increase uncertainty; more processing steps needed	Dependent on scaling factor; no improvements on vanished glaciers.

6.1 Interpolation method

As described in Section 4.1 and shown in Fig. 6**,** the NN and TtR interpolation methods performed best in the glacier surface replication tests. Especially NN interpolation can be recommended due to its simplicity and good performance. TtR interpolation can combine multiple

data types (e.g. elevation points and contour lines) and can be favoured if related datasets are used. The Spline interpolation can work well when centre points are present, but should otherwise be avoided due to unrealistic artefacts emerging from the interpolation. Kriging and IDW did not perform well for glacier surfaces. Carrivick et al. (2019, 2020, 2023) and Lee et al. (2021) have also used NN interpolation for their studies. Colucci and Žebre (2016) have used TtR whereas Glasser et al. (2011) have worked with triangular irregular networks (TINs). Pellitero et al. (2016) have included several interpolation methods (TtR, IDW, Kriging and Trend) for glacier surface reconstruction without giving a recommendation.

6.2 Interpolating the ablation area only vs. the entire glacier area

Including the accumulation area into the surface reconstruction process has a great impact on volume change estimations (Fig. 13c and 13d). For Novaya Zemlya, only reconstructing the ablation area gives about 35% lower volume changes (-5.0 km^3) for both the reconstruction with centre points and the up-scaling approach. In the Bernese Alps, the underestimation is with values between -37.5% or -10.23 km^3 (GIS reconstruction with centre point) and -27% or -6.16 km^3 (up-scaling approach) very similar. However, how much of the change in the accumulation area is due to interpolation errors and how much is real change is difficult to determine. As shown in the replication test, glacier surface elevations are overestimated by c. 5-10 m in the accumulation area, depending on the method.

For the Bernese Alps, the comparison of the reference DEM (from contour lines of the Dufour Atlas) with the swissALTI3d showed also a surface lowering and thus volume loss in the accumulation area. The difference was quantified to -7 km^3, indicating that a simple interpolation would fill up the basins too much (-10.5 km^3), that centre points are only improving the result slightly and the up-scaling approach is closest to the reference dataset (-6.2 km^3). Similarly, on Novaya Zemlya, the up-scaling approach also resulted in lower volume losses in the accumulation area. Generally, the peak in mean volume change occurs around the ELA, thus including also the areas above the ELA is important for a realistic estimation of the glacier contribution to sea level rise. Hence, delineating trim lines above the ELA when they are visible is important, but only the up-scaling approach might provide a realistic glacier surface and thus elevation change estimate in this region.

6.3 Centre points

The inclusion of centre points into the interpolation did not change the resulting surface and volume changes substantially for a larger sample of glaciers. When applying them to a small

sample of glaciers and manually filtering misclassified centre points, the method can reduce the uncertainty over wide areas in the accumulation as well as ablation area. Their inclusion is also beneficial when reconstructing piedmont glaciers which have an ablation area with a strongly convex shape and lateral moraines which are often lower than the glacier surface. More points along the cross-section could improve the ability to preserve the surface morphology, but are probably not worth the additional processing steps. In summary, we recommend using the outline points for valley glaciers and include centre points where necessary (wide glacier plateaus and piedmont glacier tongues) to better retain the glacier curvature. For glacier tongues in general, centre points only improve the reconstruction if the length changes since the LIA are smaller than the width of the glacier.

6.4 Up-scaling of recent elevation change data

Using smoothed elevation change data from Hugonnet et al. (2021) to create LIA glacier surface elevations within the modern outline and a recent DEM works well for individual glaciers and on a regional scale if calibrated with several glaciers. For climatically homogenous regions, the scaling factor (LIA dh_{factor}) is robust to the glacier sample as well as across all elevations, except the highest ones. Here, elevation change values used for the calibration of the scaling factor are close to 0 and thus the factor can reach unrealistically high values. We can recommend using a single scaling factor across all elevations. The method can also provide valuable information about the LIA surface elevation over ice caps where the traditional interpolation of moraine and trimline elevations is not possible. A glacier specific scaling factor is possible, but has limitations for very small glaciers and cannot be transferred to glaciers where the dh_{LIA} calculation from the simple surface reconstruction is not possible (e.g. ice caps). Furthermore, the method has a large potential for reducing the overestimation bias in the accumulation area since real, glacier-specific elevation values are used as an input and area changes (visible trimlines) might not always be visible. A limitation of the method is the need for LIA glacier elevation changes for the calibration of the scaling factor. These might not always be present or difficult to produce, depending on the region and glacier type. Further research is needed to determine the larger scale variability of the scaling factor.

6.5 Elevation change (rates) since the LIA compared to literature values and the recent trend

In Novaya Zemlya, the elevation change rate during the last 20 years was more than five times larger (-0.74 m a^{-1}) compared to the change rate between the LIA maximum extent (when assumed to be in 1850) and 2018 (-0.13 m a^{-1}, largely independent of the reconstruction method).

The variability of the results between the reconstruction methods is only visible in the third decimal. Most of the acceleration in thinning happened at lower elevations (>6-fold increase for elevations <450 m) with a decreasing trend towards higher elevations. Above 900 m, the dataset of Hugonnet et al. (2021) experienced lower elevation change rates than the long-term trend and even show slight elevation gains above 950 m (Fig. 15a), which might be related to errors in the dataset. Małecki (2022) analysed elevation changes between 2013 and 2016 for a small sample of glaciers covering 53 km^2 in the same region. They calculated an elevation change rate of -1.23±0.09 m a^{-1}. Ciracì et al. (2018) suggested an elevation change of -2.5 m a^{-1} below 500 m and averaged over the 2002 to 2016 period. This recent acceleration of elevation change rates for the Arctic glaciers of Novaya Zemlya indicates a strong response to recently increased temperatures and suggests that they will continue shrinking significantly over the next decade.

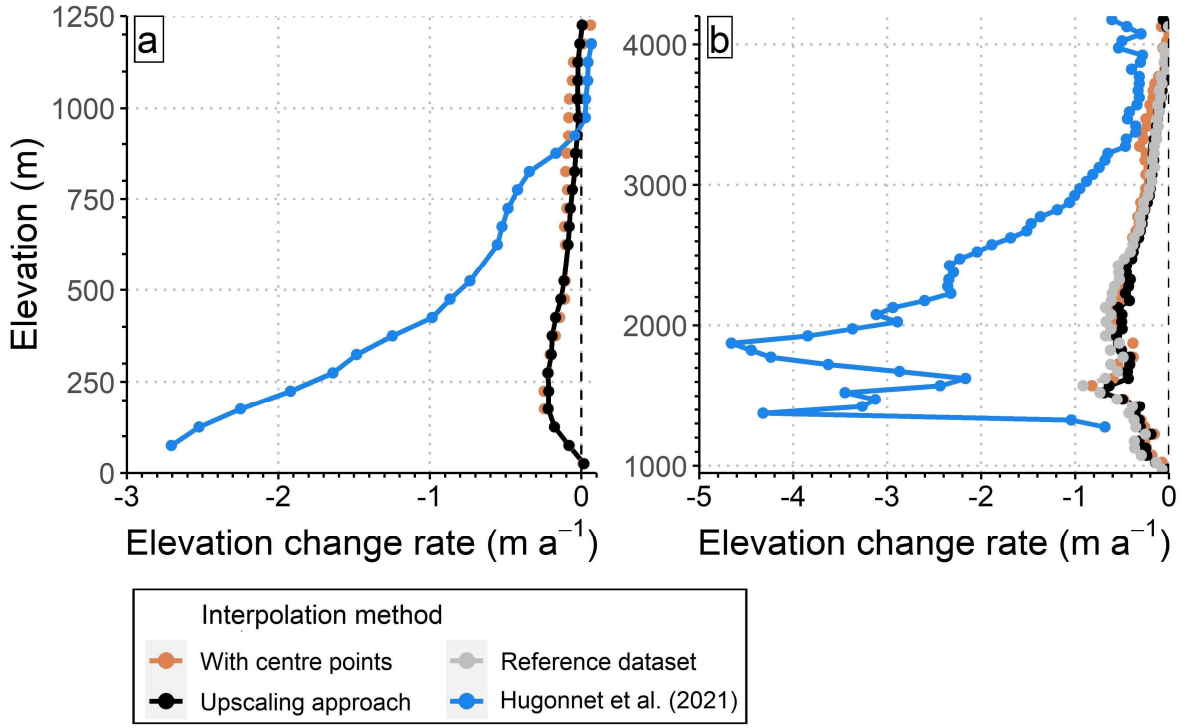

Fig. 15. Comparison of mean elevation change rates between the periods LIA to present (assumed as 1850-2018) and 2000 to 2019 (Hugonnet et al., 2021) for (a) Novaya Zemlya and (b) the Bernese Alps.

In the Bernese Alps, the obtained mean elevation change rate since the LIA maximum (≈1850) is -0.14-0.22 m a^{-1}. For some glaciers, long-term elevation change observations are available, even though not necessarily since the LIA maximum extent. For example, we have calculated a mean elevation change (using the up-scaling approach) of -54.4 m (-0.33 m a^{-1} between 1850-2016) for the Great Aletsch Glacier, whereas GLAMOS (2022) show a mean elevation change

of -77.2 m (-0.56 m a^{-1} between 1880 and 2017), i.e. considerably larger. In part, this could be due to the minimal volume change between 1850 and 1880. For the time period 1880 to 1996 and glaciers longer than 10 km, the study by Hoelzle et al. (2003) determined a mean specific mass balance of -0.27 m a^{-1} from cumulative length changes over the same time period.

Considering the strong volume loss from 1996 to 2016, our slightly higher value of -0.33 m a^{-1} is in very good agreement with this estimate. Similarly, for the lower Grindelwald Glacier, the mean elevation change from this study is -50.1 m (-0.30 m a^{-1} between 1850-2016) whereas GLAMOS (2022) published a change of -67.4 m (-0.44 m a^{-1} between 1861-2016). The volume change was calculated by GLAMOS (2022) to -6.84 km^3 (-5.68 km^3 in this study) for the Great Aletsch Glacier and -1.7 km^3 (-1.14 km^3 in this study) for the lower Grindelwald Glacier. The reasons for the lower changes in this study are inconclusive and need further investigation. The elevation change rates between 2000 and 2019 increased five to eightfold compared to the long-term trend since the LIA from this study, reaching -1.14 m a^{-1}. The regions where the elevation change rates accelerated the most are found below 1900 m (Fig. 15b), where they increased almost 11-fold (from -0.34 m a^{-1} to -3.79 m a^{-1}). Above an elevation of 3000 m, the acceleration was still more than 5-fold (from -0.10 m a^{-1} to -0.58 m a^{-1}).

The acceleration of volume change rates is less pronounced in the Bernese Alps compared to Novaya Zemlya. This is probably caused by climatic and glaciological differences. Glaciers in the Bernese Alps have generally a steeper mass balance gradient and are thus reacting faster to climatic changes (Johannesson et al., 1989). Also, glaciers in Novaya Zemlya are assumed to be cold-based or polythermal which slows the reaction to climatic changes (Małecki, 2022). Climate sensitivity also plays a major role with recent glacier melt in the Bernese Alps, being largely driven by enhanced summer melt (e.g. Zemp et al., 2015).

7. Conclusion

In this study we presented (a) an analysis of different spatial interpolation techniques when used for the reconstruction of glacier surfaces, (b) diverse sensitivity tests for the input and output datasets, (c) a new method (up-scaling) to reconstruct LIA glacier surfaces and (d) an application of the selected best methods to a sample of glaciers in two study regions (Novaya Zemlya and Bernese Alps) to determine their volume changes since the LIA along with a comparison to recent volume change rates.

The evaluation of the spatial interpolation methods revealed that the *Topo to Raster* and *Natural Neighbor* methods outperform the others (Splines, Kriging, IDW) in terms of their lower mean difference and spatial variability compared to a modern reference DEM. The sensitivity test revealed that simple interpolation of outline points works well for typical valley glaciers, but including elevations at centre points can improve curvature-related surface morphology, in particular at the scale of individual glaciers. Including elevation changes in the accumulation area has indeed a strong impact on the determined total volume changes (adding 30-50%) and should thus be included whenever possible. Of course, the higher uncertainties in this region have to be considered when calculating volume changes.

Our new reconstruction method using up-scaling of recent elevation change rates performed better compared to the simple outline point interpolation (RMSE of 26.7 vs 39.8 m) and also shows better results in the accumulation areas of valley glaciers (smaller difference to the reference dataset) and promising results for ice caps which have no trimlines indicating elevation change. However, a scaling factor is needed and its calibration requires at least the availability of some outline reconstructions for past LIA extents from geomorphology or other evidence.

The application of the new up-scaling method to the two regions (Novaya Zemlya and Bernese Alps) revealed that surface elevation (-21.1 m and -30.0 m) and glacier volume (-17% and -40.3%) have decreased significantly since the Little Ice Age and that elevation change rates have accelerated substantially over the past two decades (by a factor of 6 and 8 for the two regions, respectively) compared to the longer-term mean, even when including a larger part of the recent period. We recommend continuing the reconstruction of past glacier extents and their surfaces around the world, for example to determine past sea-level contributions of glaciers more precisely.

Data

The LIA surface elevation grids (using the up-scaling approach) can be downloaded under https://zenodo.org/records/12611033.

Acknowledgements

The work of J. R. is supported by PROTECT. This project has received funding from the European Union's Horizon 2020 research and innovation programme under grant agreement No

869304, PROTECT contribution number 95. The work of F.P. has been performed in the framework of the ESA project Glaciers_cci+ (4000127593/19/I-NB).

Authors' contributions

J. R. led the study and the writing of the paper, performed the methodological development as well as all calculations. F. P. provided ideas (e.g. for the up-scaling approach) and comments, contributed to the writing of the paper.

References

Baumann, S., Winkler, S., Andreassen, L.M., 2009. Mapping glaciers in Jotunheimen, South-Norway, during the "Little Ice Age" maximum. Cryosphere 3, 231–243. https://doi.org/10.5194/tc-3-231-2009

Benn, D.I., Evans, D.J.A., 2010. Glaciers & Glaciation, second edi. ed. Routledge, London. https://doi.org/10.5860/choice.35-6240

Benn, D.I., Hulton, N.R.J., 2010. An ExcelTM spreadsheet program for reconstructing the surface profile of former mountain glaciers and ice caps. Comput Geosci 36, 605–610. https://doi.org/10.1016/j.cageo.2009.09.016

Braithwaite, R.J., 2015. From Doktor Kurowski's Schneegrenze to our modern glacier equilibrium line altitude (ELA). Cryosphere 9, 2135–2148. https://doi.org/10.5194/tc-9-2135-2015

Braithwaite, R.J., Raper, S.C.B., 2009. Estimating equilibrium-line altitude (ELA) from glacier inventory data. Ann Glaciol 50, 127–132. https://doi.org/10.3189/172756410790595930

Carrivick, J.L., Davies, B.J., Glasser, N.F., Nývlt, D., Hambrey, M.J., 2012. Late-Holocene changes in character and behaviour of land-terminating glaciers on James Ross Island, Antarctica. Journal of Glaciology 58, 1176–1190. https://doi.org/10.3189/2012JoG11J148

Carrivick, J.L., Boston, C.M., King, O., James, W.H.M., Quincey, D.J., Smith, M.W., Grimes, M., Evans, J., 2019. Accelerated volume loss in glacier ablation zones of NE Greenland , Little Ice Age to present. Geophys Res Lett 46, 1476–1484. https://doi.org/10.1029/2018GL081383

Carrivick, J.L., James, W.H.M., Grimes, M., Sutherland, J.L., Lorrey, A.M., 2020. Ice thickness and volume changes across the Southern Alps, New Zealand, from the little ice age to present. Sci Rep 10, 1–10. https://doi.org/10.1038/s41598-020-70276-8

Carrivick, J.L., Andreassen, L.M., Nesje, A., Yde, J.C., 2022. A reconstruction of Jostedalsbreen during the Little Ice Age and geometric changes to outlet glaciers since then. Quat Sci Rev 284, 107501. https://doi.org/10.1016/j.quascirev.2022.107501

Carrivick, J.L., Boston, C.M., Sutherland, J.L., Pearce, D., Armstrong, H., Bjørk, A., Kjeldsen, K.K., Abermann, J., Oien, R.P., Grimes, M., James, W.H.M., Smith, M.W., 2023. Mass Loss of Glaciers and Ice Caps Across Greenland Since the Little Ice Age. Geophys Res Lett 50. https://doi.org/10.1029/2023GL103950

Carr, J.R., Stokes, C., Vieli, A., 2014. Recent retreat of major outlet glaciers on Novaya Zemlya, Russian Arctic, influenced by fjord geometry and sea-ice conditions. Journal of Glaciology 60, 155–170. https://doi.org/10.3189/2014JoG13J122

Ciracì, E., Velicogna, I., Sutterley, T.C., 2018. Mass balance of Novaya Zemlya archipelago, Russian high arctic, using time-variable gravity from GRACE and altimetry data from ICESat and CryoSat-2. Remote Sens (Basel) 10, 1–26. https://doi.org/10.3390/rs10111817

Colucci, R.R., Žebre, M., 2016. Late Holocene evolution of glaciers in the southeastern Alps. J Maps 12, 289–299. https://doi.org/10.1080/17445647.2016.1203216

[dataset] ESRI, 2023. "World Imagery" [basemap]. scale not given. "world imagery vivid" [WWW Document]. URL https://services.arcgisonline.com/ArcGIS/rest/services/World_Imagery/MapServer

Farinotti, D., Huss, M., Bauder, A., Funk, M., Truffer, M., 2009. A method to estimate the ice volume and ice-thickness distribution of alpine glaciers. Journal of Glaciology 55, 422–430. https://doi.org/10.3189/002214309788816759

Farinotti, D., Huss, M., Fürst, J.J., Landmann, J., Machguth, H., Maussion, F., Pandit, A., 2019. A consensus estimate for the ice thickness distribution of all glaciers on Earth. Nat Geosci 12, 168–173. https://doi.org/10.1038/s41561-019-0300-3

Freudiger, D., Mennekes, D., Seibert, J., Weiler, M., 2018. Historical glacier outlines from digitized topographic maps of the Swiss Alps. Earth Syst Sci Data 10, 805–814. https://doi.org/10.5194/essd-10-805-2018

Geyman, E.C., J. J. van Pelt, W., Maloof, A.C., Aas, H.F., Kohler, J., 2022. Historical glacier change on Svalbard predicts doubling of mass loss by 2100. Nature 601, 374–379. https://doi.org/10.1038/s41586-021-04314-4

Girod, L., Ivar Nielsen, N., Couderette, F., Nuth, C., Kääb, A., 2018. Precise DEM extraction from Svalbard using 1936 high oblique imagery. Geoscientific Instrumentation, Methods and Data Systems 7, 277–288. https://doi.org/10.5194/gi-7-277-2018

[dataset] GLAMOS, 2022. Swiss Glacier Volume Change, release 2022. https://doi.org/10.18750/volumechange.2022.r2022.zip

Glasser, N.F., Harrison, S., Jansson, K.N., Anderson, K., Cowley, A., 2011. Global sea-level contribution from the Patagonian Icefields since the Little Ice Age maximum. Nat Geosci 4, 303–307. https://doi.org/10.1038/ngeo1122

Grant, K.L., Stokes, C.R., Evans, I.S., 2009. Identification and characteristics of surge-type glaciers on Novaya Zemlya, Russian Arctic. Journal of Glaciology 55, 960–972. https://doi.org/10.3189/002214309790794940

Grove, J.M., 2008. The Little Ice Age. Prog Phys Geogr 32, 103–106. https://doi.org/10.1177/0309133308089501

Haeberli, W., Hoelzle, M., 1995. Application of inventory data for estimating characteristics of and regional climate-change effects on mountain glaciers: a pilot study with the European Alps. Ann Glaciol 21, 206–212. https://doi.org/10.3189/s0260305500015834

Hannesdóttir, H., Björnsson, H., Pálsson, F., Guðmundsson, S., 2015. Variations of southeast Vatnajökull ice cap (Iceland) 1650 – 1900 and reconstruction of the glacier surface geometry at the little ice age maximum. Geografiska Annaler 97, 237–264. https://doi.org/10.1111/geoa.12064

Hoelzle, M., Haeberli, W., Dischl, M., Peschke, W., 2003. Secular glacier mass balances derived from cumulative glacier length changes. Glob Planet Change 36, 295–306. https://doi.org/10.1016/S0921-8181(02)00223-0

Horwath, M., Gutknecht, B.D., Cazenave, A., Palanisamy, H.K., Marti, F., Marzeion, B., Paul, F., Le Bris, R., Hogg, A.E., Otosaka, I., Shepherd, A., Döll, P., Cáceres, D., Müller Schmied, H., Johannessen, J.A., Nilsen, J.E.Ø., Raj, R.P., Forsberg, R., Sandberg Sørensen, L., Barletta, V.R., Simonsen, S.B., Knudsen, P., Andersen, O.B., Ranndal, H., Rose, S.K., Merchant, C.J., Macintosh, C.R., Von Schuckmann, K., Novotny, K., Groh, A., Restano, M., Benveniste, J., 2022. Global sea-level budget and ocean-mass budget, with a focus on advanced data products and uncertainty characterisation. Earth Syst Sci Data 14, 411–447. https://doi.org/10.5194/essd-14-411-2022

Hugonnet, R., McNabb, R., Berthier, E., Menounos, B., Nuth, C., Girod, L., Farinotti, D., Huss, M., Dussaillant, I., Brun, F., Kääb, A., 2021. Accelerated global glacier mass loss in the early twenty-first century. Nature 592, 726–731. https://doi.org/10.1038/s41586-021-03436-z

Huss, M., Jouvet, G., Farinotti, D., Bauder, A., 2010. Future high-mountain hydrology: A new parameterization of glacier retreat. Hydrol Earth Syst Sci 14, 815–829. https://doi.org/10.5194/hess-14-815-2010

Hutchinson, M.F., 1989. A new procedure for gridding elevation and stream line data with automatic removal of spurious pits. J Hydrol (Amst) 106, 211–232. https://doi.org/10.1016/0022-1694(89)90073-5

Johannesson, T., Raymond, C., Waddington, E., 1989. Time-scale for adjustment of glaciers to changes in mass balance. Journal of Glaciology 35, 355–369. https://doi.org/10.1017/S002214300000928X

Jouvet, G., Huss, M., Blatter, H., Picasso, M., Rappaz, J., 2009. Numerical simulation of Rhonegletscher from 1874 to 2100. J Comput Phys 228, 6426–6439. https://doi.org/10.1016/j.jcp.2009.05.033

Jouvet, G., 2022. Inversion of a Stokes ice flow model emulated by deep learning. Journal of Glaciology 1–14. https://doi.org/https:// doi.org/10.1017/jog.2022.41

Khan, S.A., Kjeldsen, K.K., Kjær, K.H., Bevan, S., Luckman, A., Bjørk, A.A., Korsgaard, N.J., Box, J.E., van den Broeke, M., van Dam, T.M., Fitzner, A., 2014. Glacier dynamics at Helheim and Kangerdlugssuaq glaciers, southeast Greenland, since the Little Ice Age. Cryosphere 8, 1497–1507. https://doi.org/10.5194/tc-8-1497-2014

Kienholz, C., Rich, J.L., Arendt, A.A., Hock, R., 2014. A new method for deriving glacier centerlines applied to glaciers in Alaska and northwest Canada. Cryosphere 8, 503–519. https://doi.org/10.5194/tc-8-503-2014

Kurowski, L., 1891. Die Höhe der Schneegrenze mit besonderer Berücksichtigung der Finsteraarhorn-Gruppe. Berliner geowissenschaftliche Abhandlungen 5, 119–160.

Lee, E., Carrivick, J.L., Quincey, D.J., Cook, S.J., James, W.H.M., Brown, L.E., 2021. Accelerated mass loss of Himalayan glaciers since the Little Ice Age. Sci Rep 11, 1–8. https://doi.org/10.1038/s41598-021-03805-8

Linsbauer, A., Paul, F., Haeberli, W., 2012. Modeling glacier thickness distribution and bed topography over entire mountain ranges with glabtop: Application of a fast and robust approach. J Geophys Res Earth Surf 117, 1–17. https://doi.org/10.1029/2011JF002313

[dataset] Linsbauer, A., Huss, M., Hodel, E., Bauder, A., Fischer, M., Weidmann, Y., Bärtschi, H., Schmassmann, E., 2021. The New Swiss Glacier Inventory SGI2016 : From a Topographical to a Glaciological Dataset. Front Earth Sci (Lausanne) 9, 1–22. https://doi.org/10.3389/feart.2021.704189

[dataset] Maisch, M., Wipf, A., Denneler, B., Battaglia, J., Benz, C., 2000. Die Gletscher der Schweizer Alpen: Gletscherhochstand 1850, aktuelle Vergletscherung, Gletscherschwundszenarien, in: Schlussbericht NFP 31, Second Edition. Hochschulverlag ETH Zurich, Zurich, p. 373p. https://doi.glamos.ch/data/inventory/inventory_sgi1850_r1992.html

Małecki, J., 2022. Recent contrasting behaviour of mountain glaciers across the European High Arctic revealed by ArcticDEM data. Cryosphere 16, 2067–2082. https://doi.org/10.5194/tc-16-2067-2022

Marzeion, B., Jarosch, A.H., Hofer, M., 2012. Past and future sea-level change from the surface mass balance of glaciers. Cryosphere 6, 1295–1322. https://doi.org/10.5194/tc-6-1295-2012

Maussion, F., Butenko, A., Champollion, N., Dusch, M., Eis, J., Fourteau, K., Gregor, P., Jarosch, A.H., Landmann, J., Oesterle, F., Recinos, B., Rothenpieler, T., Vlug, A., Wild, C.T., Marzeion, B., 2019. The Open Global Glacier Model (OGGM) v1.1. Geosci Model Dev 12, 909–931. https://doi.org/10.5194/gmd-12-909-2019

Midgley, N.G., Tonkin, T.N., 2017. Reconstruction of former glacier surface topography from archive oblique aerial images. Geomorphology 282, 18–26. https://doi.org/10.1016/j.geomorph.2017.01.008

Millan, R., Mouginot, J., Rabatel, A., Morlighem, M., 2022. Ice velocity and thickness of the world's glaciers. Nat Geosci 15, 124–129. https://doi.org/10.1038/s41561-021-00885-z

Mölg, N., Bolch, T., 2017. Structure-from-motion using historical aerial images to analyse changes in glacier surface elevation. Remote Sens 9, 1–17. https://doi.org/10.3390/rs9101021

Oppenheimer, M., Glavovic, J., Hinkel, J., van de Wal, R., Magnan, A.K., Abd-Elgawad, A., Cai, R., Cifuentes-Jara, M., DeConto, R.M., Ghosh, T., Hay, J., Isla, F., Marzeion, B., Meyssignac, B., Sebesvari, Z., 2019. Sea level rise and implications for low-lying islands, coasts and communities, in: Pörtner, H.-O., Roberts, D.C., Masson-Delmotte, V., Zhai, P., Tignor, M., Poloczanska, E., Mintenbeck, K., Alegría, A., Nicolai, M., Okem, A., Petzold, J., Rama, B., Weyer, N.M. (Eds.), IPCC Special Report on the Ocean and Cryosphere in a Changing Climate. Cambridge University Press, Cambridge, UK and New York, USA, pp. 321–446. https://doi.org/https://doi.org/10.1017/9781009157964.006

Paul, F., 2010. The influence of changes in glacier extent and surface elevation on modeled mass balance. The Cryosphere 4, 569–581. https://doi.org/10.5194/tc-4-569-2010

Pellitero, R., Rea, B.R., Spagnolo, M., Bakke, J., Hughes, P., Ivy-Ochs, S., Lukas, S., Ribolini, A., 2015. A GIS tool for automatic calculation of glacier equilibrium-line altitudes. Comput Geosci 82, 55–62. https://doi.org/10.1016/j.cageo.2015.05.005

Pellitero, R., Rea, B.R., Spagnolo, M., Bakke, J., Ivy-Ochs, S., Frew, C.R., Hughes, P., Ribolini, A., Lukas, S., Renssen, H., 2016. GlaRe, a GIS tool to reconstruct the 3D surface of palaeoglaciers. Comput Geosci 94, 77–85. https://doi.org/10.1016/j.cageo.2016.06.008

Plummer, M.A., Phillips, F.M., 2003. A 2-D numerical model of snow/ice energy balance and ice flow for paleoclimatic interpretation of glacial geomorphic features. Quat Sci Rev 22, 1389–1406. https://doi.org/10.1016/S0277-3791(03)00081-7

[dataset] Porter, C., Morin, P., Howat, I., Noh, M.-J., Bates, B., Peterman, K., Keesey, S., Schlenk, M., Gardiner, J., Tomko, K., Willis, M., Kelleher, C., Cloutier, M., Husby, E., Foga, S., Nakamura, H., Platson, M., Wethington Jr., M., Williamson, C., Bauer, G., Enos, J., Arnold, G., Kramer, W., Becker, P., Doshi, A., D'Souza, C., Cummens, P., Laurier, F., Bojesen, M.A.-N.S.F., 2018. ArcticDEM, Version 3. https://doi.org/doi:10.7910/DVN/OHHUKH

Raper, S.C.B., Braithwaite, R.J., 2009. Glacier volume response time and its links to climate and topography based on a conceptual model of glacier hypsometry. Cryosphere 3, 183–194. https://doi.org/10.5194/tc-3-183-2009

Rastner, P., Strozzi, T., Paul, F., 2017. Fusion of multi-source satellite data and DEMs to create a new glacier inventory for Novaya Zemlya. Remote Sens (Basel) 9, 1–18. https://doi.org/10.3390/rs9111122

Rea, B.R., Evans, D.J.A., 2007. Quantifying climate and glacier mass balance in north Norway during the Younger Dryas. Palaeogeogr Palaeoclimatol Palaeoecol 246, 307–330. https://doi.org/10.1016/j.palaeo.2006.10.010

Reinthaler, J., Paul, F., 2023. Using a Web Map Service to map Little Ice Age glacier extents at regional scales. Ann Glaciol 1–19. https://doi.org/https://doi.org/10.1017/aog.2023.39

Schwitter, M.P., Raymond, C.F., 1993. Changes in the longitudinal profiles of glaciers during advance and retreat. Journal of Glaciology 39, 582–590. https://doi.org/10.1017/S0022143000016476

[dataset] Swisstopo, 2023. Digital Dufour Atlas. https://www.swisstopo.admin.ch/en/geo-data/maps/historical/dufour.html

Weber, P., Andreassen, L.M., Boston, C.M., Lovell, H., Kvarteig, S., 2020. An ~1899 glacier inventory for Nordland, northern Norway, produced from historical maps. Journal of Glaciology 66, 259–277. https://doi.org/10.1017/jog.2020.3

Werder, M.A., Huss, M., Paul, F., Dehecq, A., Farinotti, D., 2020. A Bayesian ice thickness estimation model for large-scale applications. Journal of Glaciology 66, 137–152. https://doi.org/10.1017/jog.2019.93

Wipf, A., 1999. Die Gletscher der Berner, Waadtländer und nördlichen Walliser Alpen (Dissertation). University of Zurich.

Wolken, G.J., England, J.H., Dyke, A.S., 2005. Re-Evaluating the Relevance of Vegetation Trimlines in the Canadian Arctic as an Indicator of Little Ice Age Paleoenvironments. Arctic 58, 341–353. https://doi.org/10.14430/arctic448

Zeeberg, J.J., Forman, S.L., 2001. Changes in glacier extent on north Novaya Zemlya in the twentieth century. Holocene 11, 161–175. https://doi.org/10.1191/095968301676173261

Zemp, M., Frey, H., Gärtner-Roer, I., Nussbaumer, S.U., Hoelzle, M., Paul, F., Haeberli, W., Denzinger, F., Ahlstrøm, A.P., Anderson, B., Bajracharya, S., Baroni, C., Braun, L.N., Càceres, B.E., Casassa, G., Cobos, G., Dàvila, L.R., Delgado Granados, H., Demuth, M.N., Espizua, L., Fischer, A., Fujita, K., Gadek, B., Ghazanfar, A., Hagen, J.O., Holmlund, P., Karimi, N., Li, Z., Pelto, M., Pitte, P., Popovnin, V. V., Portocarrero,

C.A., Prinz, R., Sangewar, C. V., Severskiy, I., Sigurdsson, O., Soruco, A., Usubaliev, R., Vincent, C., 2015. Historically unprecedented global glacier decline in the early 21st century. Journal of Glaciology 61, 745–762. https://doi.org/10.3189/2015JoG15J017

Zemp, M., Huss, M., Thibert, E., Eckert, N., McNabb, R., Huber, J., Barandun, M., Machguth, H., Nussbaumer, S.U., Gärtner-Roer, I., Thomson, L., Paul, F., Maussion, F., Kutuzov, S., Cogley, J.G., 2019. Global glacier mass changes and their contributions to sea-level rise from 1961 to 2016. Nature 568, 382–386. https://doi.org/10.1038/s41586-019-1071-0

Zumbühl, H.J., Holzhauser, H., 1988. Alpengletscher in der Kleinen Eiszeit. Die Alpen, Sonderheft zum 125 jährigen Jubiläum des SAC 65, 129–322.

Zumbühl, H.J., Nussbaumer, S.U., 2018. Little ice age glacier history of the central and western alps from pictorial documents. Geographical Research Letters 44, 115–136. https://doi.org/10.18172/cig.3363

Zumbühl, H.J., Nussbaumer, S.U., Holzhauser, H., Wolf, R., 2016. Die Grindelwaldgletscher – Kunst und Wissenschaft. Haupt-Verlag, Bern.

Assessment of methods for reconstructing Little Ice Age glacier surfaces on the examples of Novaya Zemlya and the Swiss Alps

Johannes Reinthaler[1], Frank. Paul[1]
[1] Department of Geography, University of Zurich, Zurich, Switzerland
E-mail: johannes.reinthaler@geo.uzh.ch

Supplement material

Content:

1. GIS-based LIA surface reconstruction processing steps

1. "Generate points along lines" for LIA and modern glacier outline (90 m distance)
2. "Extract Multi Values to Points" with the elevation information along the LIA outline
3. Use the centerlines and "Generate Transects along the line" with a distance of 90 m and a length of 10 m.
4. Add a unique ID to each cross-section; add glacier ID to centerlines.
5. Extend cross sections to 1. Modern outline and 2. LIA outline (Python code, available upon request).
6. Delete identical modern and LIA cross-sections (no observed elevation change) and review cross sections and delete unrealistic, and extremely long lines.
7. Create "Intersect" points of LIA outline/modern outline and centreline with the cross-sections.
8. "Create routes" of outline intersection points to split points into left and right. Use glacier ID as a route identifier field.
9. "Locate Features Along Routes" to outline intersection points.
10. "Join" route distance values to outline intersection points using unique ID (positive values are on one side, negative on the other).
11. "Extract Multi Values to Points" from DEM to outline intersection points.
12. Calculate the elevation difference (dh_m) of each pair of outline intersection points (LIA & modern) for both sides along the cross-section (Eq. 1):

$$dh_{m\ each\ side} = Outline\ elevation_{LIA} - Outline\ elevation_{modern} \quad (1)$$

13. Add dh_m centre (average of both sides) to centre point elevation from DEM (Eq.2):

$$LIA_{elevation} = Centre_{elevation} + \frac{(dh_m right + dh_m left)}{2} \quad (2)$$

14. Delete centre points where no dh was calculated (where LIA and modern outlines are identical).
15. Interpolate surface using LIA outline and centre points.

2. Up-scaling of recent elevation change data processing steps

2.1 Test sensitivity and calculation of scaling factor

1. Set areas with positive elevation change rate in the Hugonnet et al. (2021) dataset (dh_h) [m a^{-1}] to 0.
2. Create a raster with regional mean values of dh_h (dh_h mean elevation) and dh_{LIA} (dh_{LIA} mean elevation) [m] per 50 m elevation bin
3. Calculate the scaling factor (LIA dh_{factor}) with different combinations of cell-based and regional means. Do this for five samples go glaciers (split 80:20) with the 20% not repeating itself, evaluated mean differences and spread:
    a. Calibrated with mean dh_h and cell-based dh_{LIA} (Eq. 3; red & blue dots in Fig. 11)

$$LIA\ \mathrm{dh_{factor}}1 = \frac{\mathrm{dh_{LIA}}}{dh_h\ mean\ elevation} \quad (3)$$

b. Calibrated with cell-based dh_h and mean dh_{LIA} (Eq. 4; black & orange dots in Fig. 11)

$$\text{LIA } dh_{factor}2 = \frac{dh_{LIA}\ mean\ elevation}{dh_h} \quad (4)$$

4. Calculate the scaling factor (LIA dh_{factor}) as median values of cell-based dh_h and dh_{LIA} (Eq. 5; dashed vertical lines in Fig. 11):

$$\text{median (LIA } dh_{factor}) = \text{median}(\frac{dh_{LIA}}{dh_h}) \quad (5)$$

2.2 Calculate the LIA surface using glacier-specific elevation change gradients

1. Form Hugonnet et al. (2021) dataset calculate two linear regression function of elevation change with elevation for each glacier (mean elevation as breaking point). Extract slope (a) and intercept (b) parameters for each regression line.
2. Create rasters for a and b values (a1 and b1 for ablation area, a2 and b2 for accumulation area).
3. Apply function to get predicted elevation change values (Eq. 6):

$$dh_h\ predict\ =\ if\ DEM < mean\ elevation, a1 * DEM + b1, else\ a2 * DEM + b2 \quad (6)$$

4. Use the median scaling factor which serves as a regional applicable scaling factor (median dh_{factor}).
5. Calculate LIA surface elevation for the area within the modern extent (Eq. 7):

$$LIA_{elevation} = \text{DEM} - (dh_h\ predict * \text{median}(\text{LIA } dh_{factor})) \quad (7)$$

6. Convert LIA elevation raster to point elevations, combine with outlines elevation points and interpolate the complete LIA surface.

3. Supplementary figures

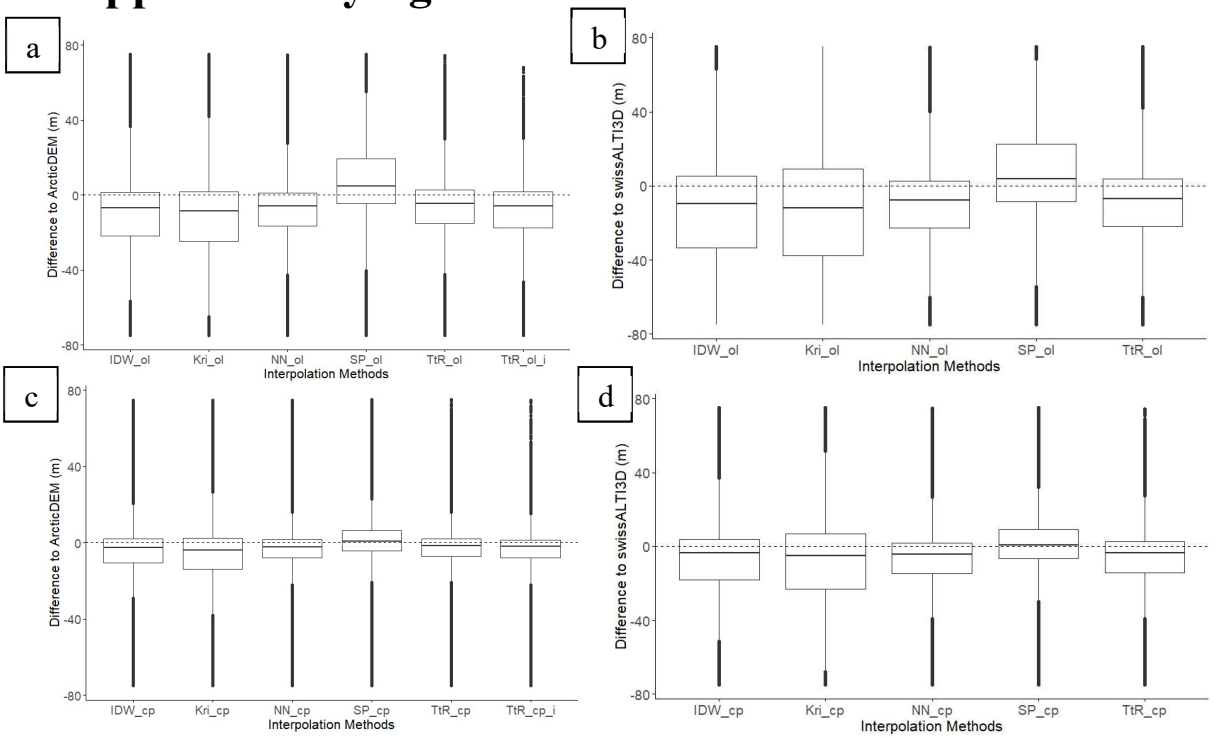

Figure S 1: Boxplot of the analysed interpolation methods for Novaya Zemlya without a) and with c) centre points and the Bernese Alps (c and d, respectively).

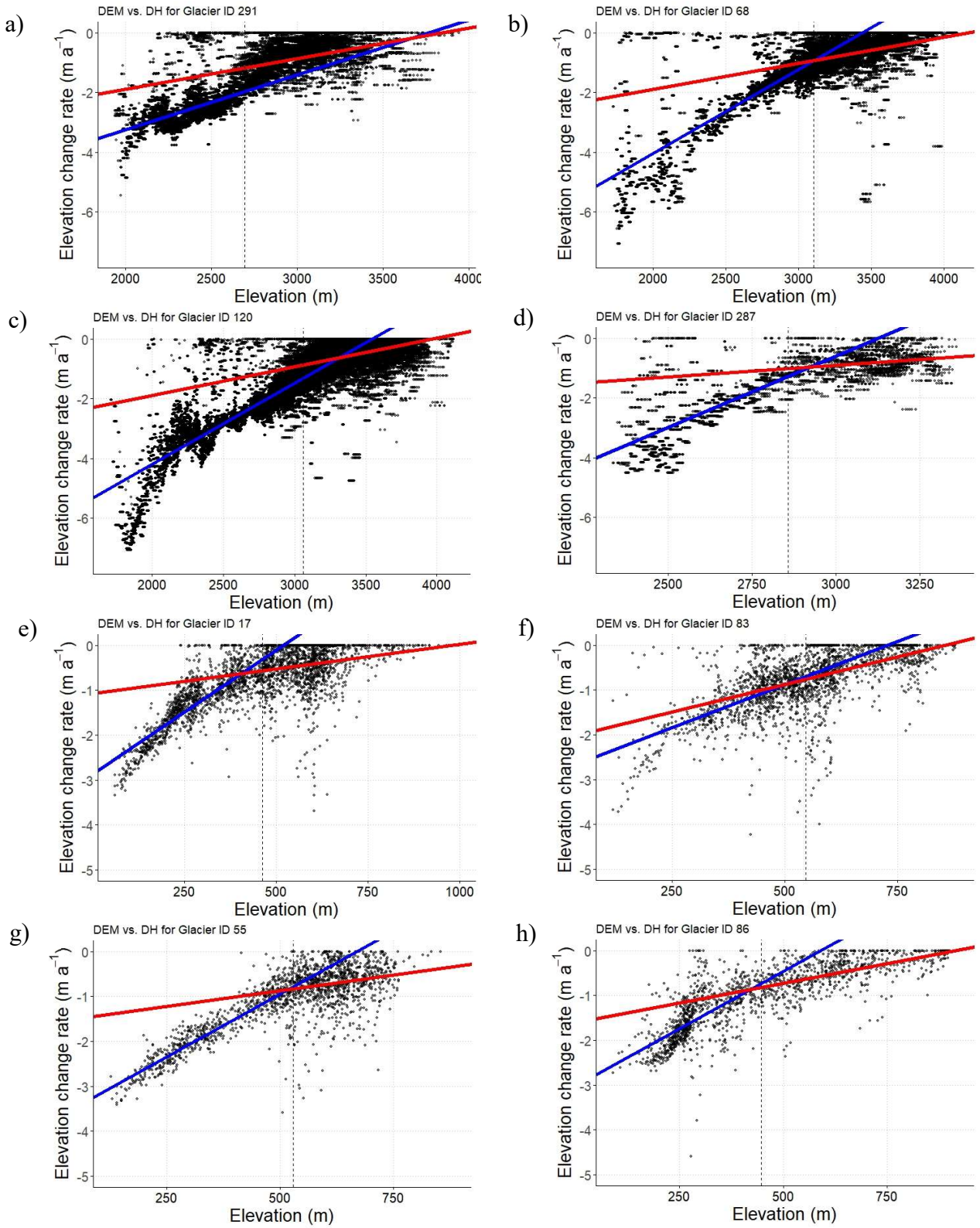

Figure S 2: Examples of bilinear elevation change gradients for both regions (a-d = Bernese Alps, e-h = Novaya Zemlya). The blue line indicated the elevation change rate gradient for the ablation area and the red line for the accumulation area. The dashed vertical line shows the mean elevation. (a = Unteraar glacier; b = Fiescher glacier; c = Great Aletsch glacier; d = Oberaar glacier; e = RGI60-09.00254; f = RGI60-09.00253; g = RGI60-09.00264 & RGI60-09.00266; h = RGI60-09.00153 & RGI60-09.00443;

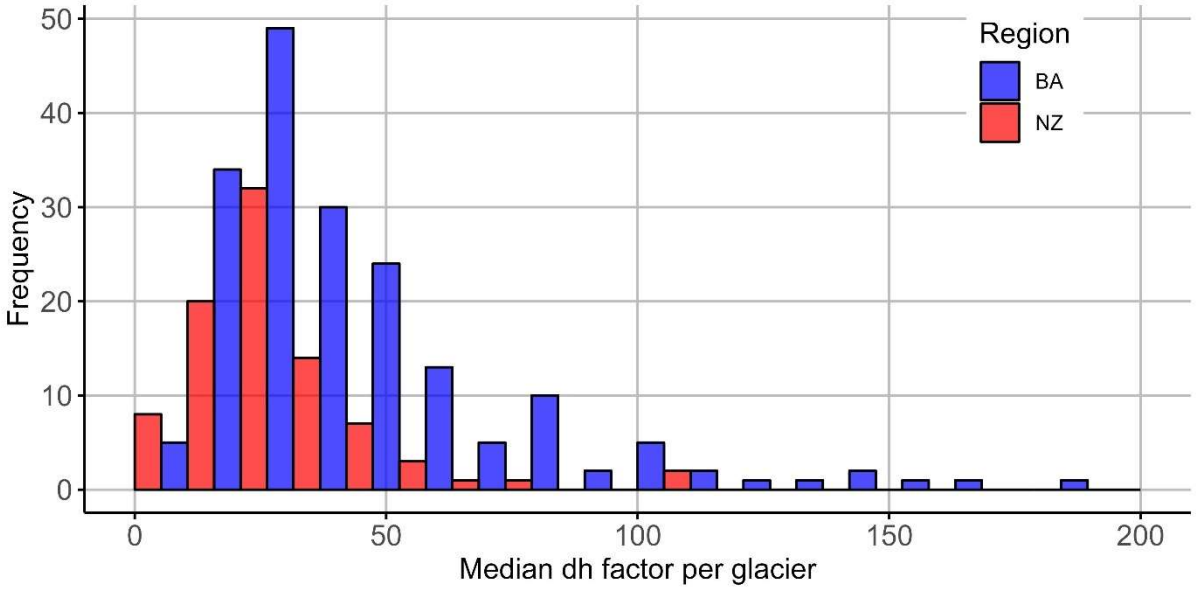

Figure S 3: Histogram of median scaling factor per glacier for both regions.

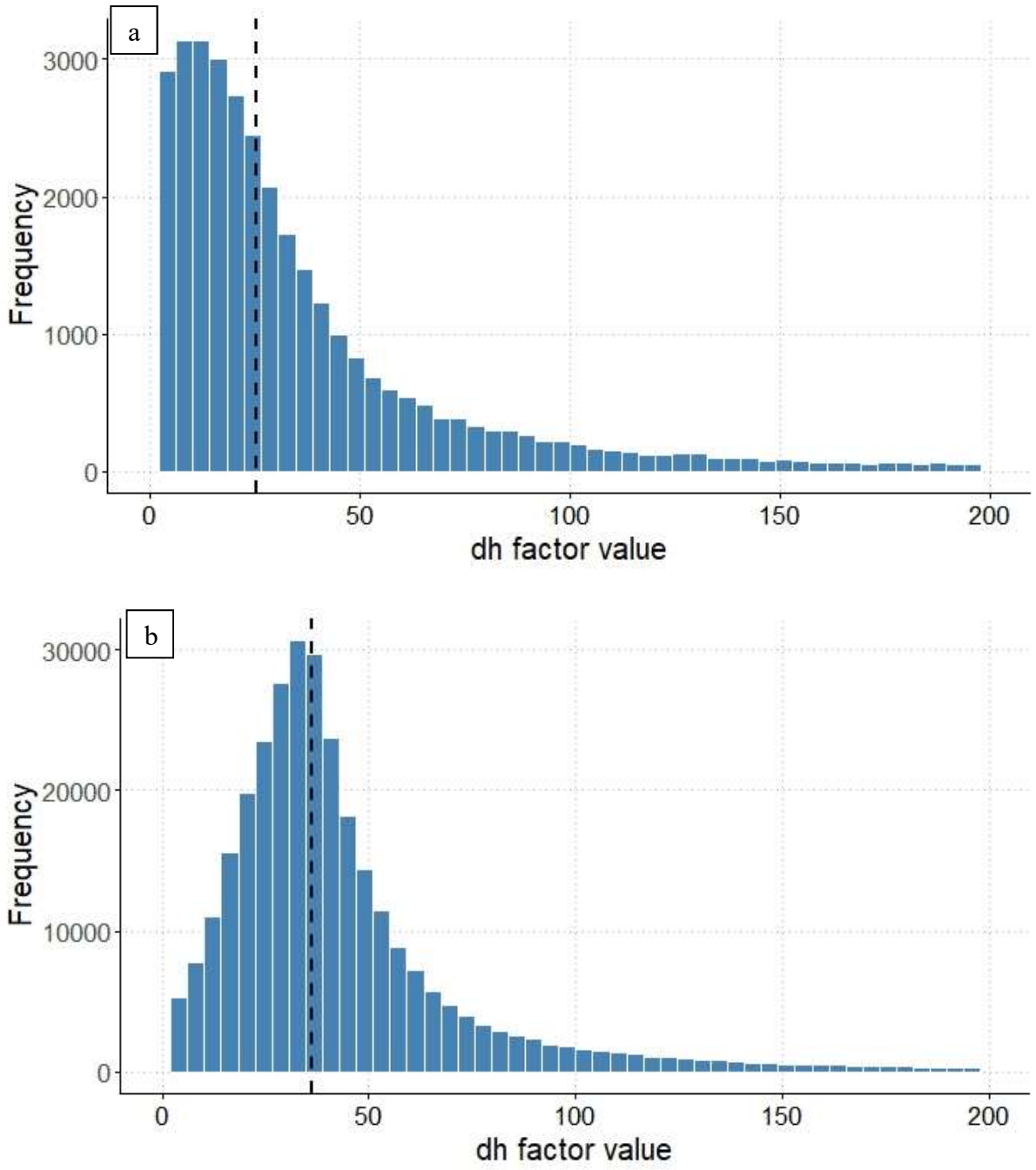

Figure S 4: Histogram of scaling factor a) on Novaya Zemlya and b) in the Bernese Alps. The dashed vertical line indicates the median value.

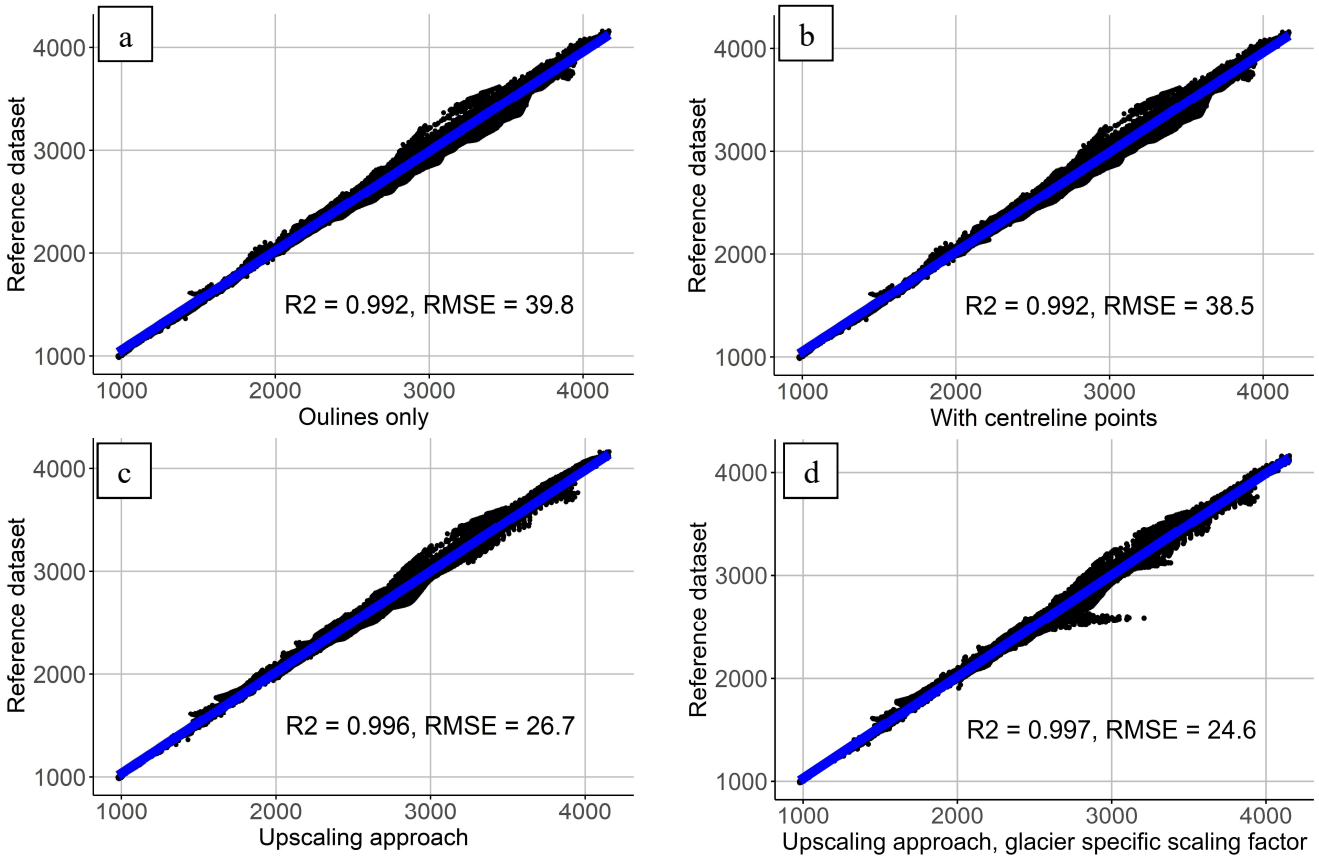

Figure S 5: Scatter plot comparing the reference dataset elevation with the LIA reconstruction using a) the outline points only, b) including centreline points, c) the up-scaling approach and d) the up-scaling approach with a glacier specific scaling factor.

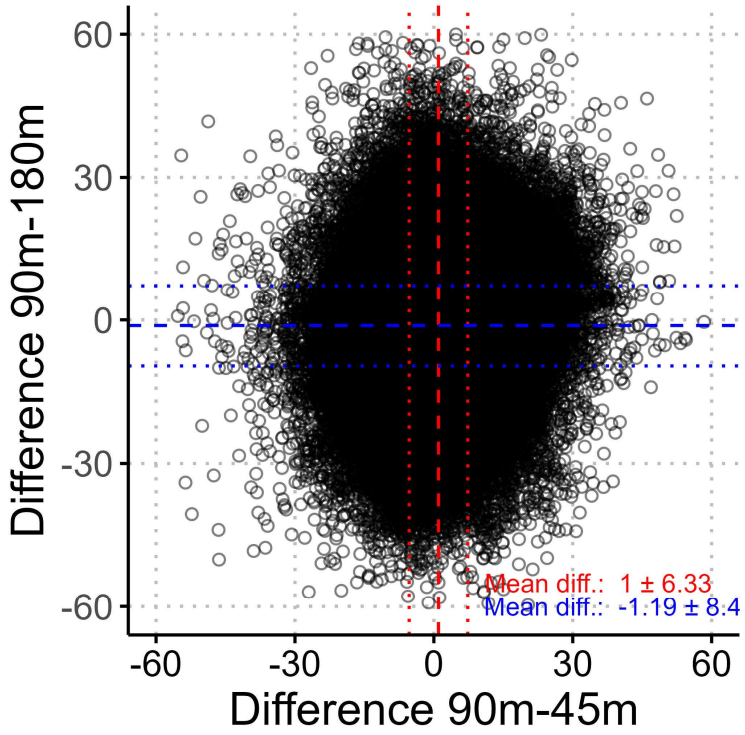

Figure S 6: Difference of using 90 m sampling distance vs 180m (y-axis) and 45 m (x-axis) Values and lines indicate the mean (dashed) and standard deviation (dotted).45 m spacing produced the lowest surface elevation and 180 m the highest.

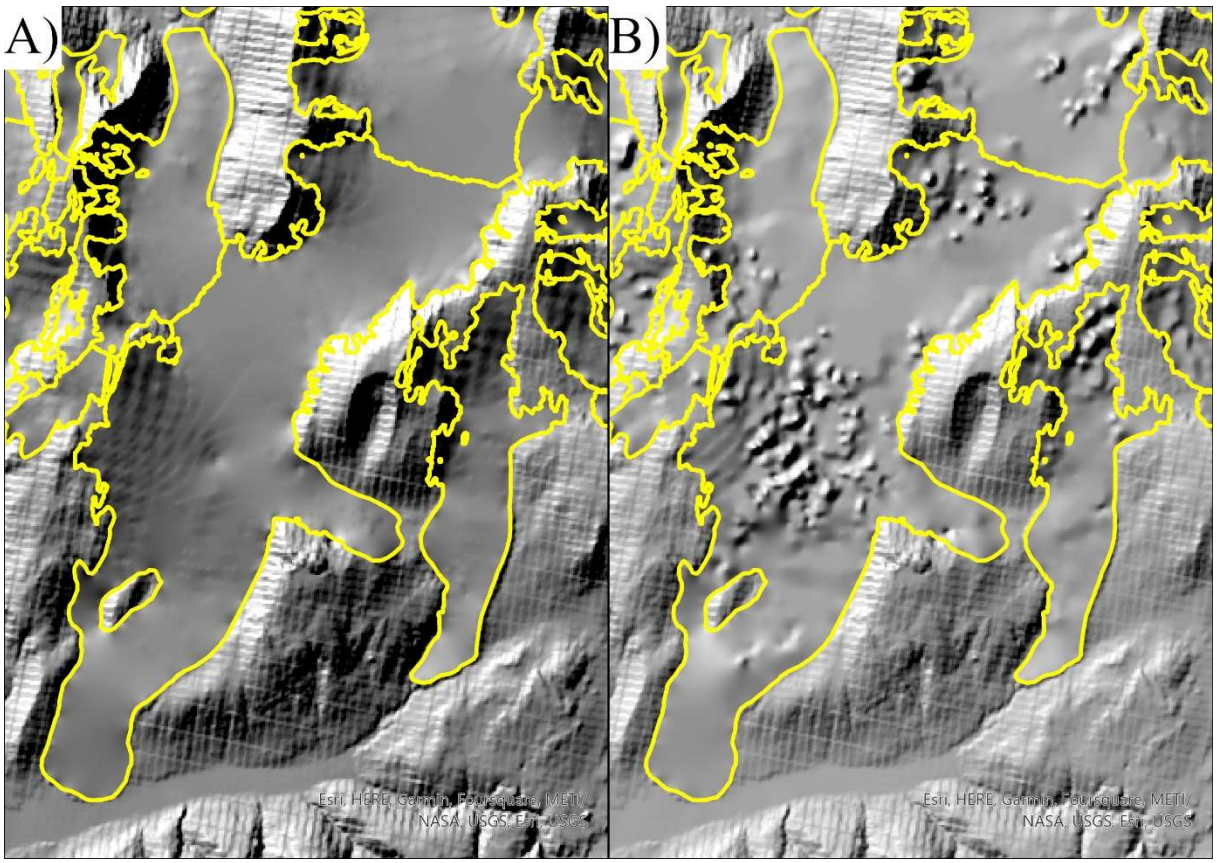

Figure S 7: Up-scaling approach LIA reconstruction on Novaya Zemlya (73.007° N, 54.575° E) using A) dh_h values from bilinear regression and B) raw input data. Note the amplification of noise when using the raw elevation change data.